

Reliable algorithm selection for machine learning-guided design

Clara Fannjiang and Ji Won Park

Prescient Design, Genentech

Abstract

Algorithms for machine learning-guided design, or *design algorithms*, use machine learning-based predictions to propose novel objects with desired property values. Given a new design task—for example, to design novel proteins with high binding affinity to a therapeutic target—one must choose a design algorithm and specify any hyperparameters and predictive and/or generative models involved. How can these decisions be made such that the resulting designs are successful? This paper proposes a method for *design algorithm selection*, which aims to select design algorithms that will produce a distribution of design labels satisfying a user-specified success criterion—for example, that at least ten percent of designs’ labels exceed a threshold. It does so by combining designs’ predicted property values with held-out labeled data to reliably forecast characteristics of the label distributions produced by different design algorithms, building upon techniques from prediction-powered inference [2]. The method is guaranteed with high probability to return design algorithms that yield successful label distributions (or the null set if none exist), if the density ratios between the design and labeled data distributions are known. We demonstrate the method’s effectiveness in simulated protein and RNA design tasks, in settings with either known or estimated density ratios.

1 Design algorithm selection

Machine learning-guided design aims to propose novel objects, or *designs*, that exhibit desired values of a property of interest by consulting machine learning-based predictions of the property in place of costly and time-consuming measurements. The approach has been used to design novel enzymes that efficiently catalyze reactions of interest [18], photoreceptors with unprecedented light sensitivity for optogenetics [4], and antibodies with enhanced binding affinity to therapeutic targets [21], among many other applications. The methods used in such efforts, which we call *design algorithms*, are varied. Some entail sampling from a generative model that upweights objects with promising predictions [8, 7]; others start with initial candidates and iteratively introduce modifications that yield more desirable predictions [10, 46]. To propose designs, one must choose among these design algorithms. Many have consequential hyperparameter(s) that must be set, such as those that navigate a trade-off between departing from training data to achieve unprecedented predicted values and staying close enough that those predictions can be trusted [7, 21, 54]. One must also specify the predictive model that the design algorithm consults, as well as any generative model it may involve. These decisions collectively yield a *design algorithm configuration*, or *configuration* for short—for example, the design algorithm AdaLead [40] using the hyperparameter settings $r = 0.2, \mu = 0.02, \kappa = 0.05$ and a ridge regression predictive model. The choice of the configuration dictates the resulting designs, and, consequently, whether the design effort succeeds or fails. Specifically, we say that a configuration is *successful* if it produces a distribution of design labels that satisfies a user-specified *success criterion*—for example, that at least ten percent of the design labels exceed some threshold. In this paper, we propose a solution to the problem of *design algorithm selection*:

How can one select a design algorithm configuration that is guaranteed to be successful?

To anticipate whether a configuration will be successful, one can examine predicted property values for designs that it produces. However, these predictions can be particularly error-prone, as design algorithms often produce distributions of designs shifted away from the training data in order to achieve unprecedented predicted values [14]. We propose a method for design algorithm selection that combines predictions for designs with labeled data held out from training, in a way that corrects for these errors and enables theoretical

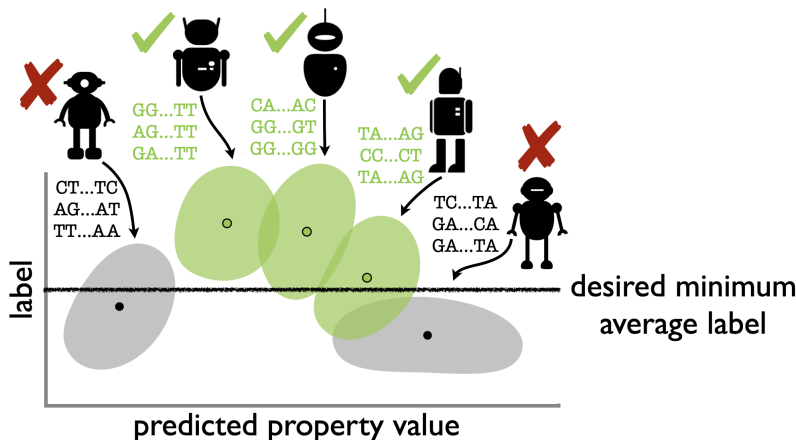


Figure 1: **Design algorithm selection.** Different design algorithm configurations (shown as robots) produce different distributions of designs (*e.g.*, biological sequences). Distributions of designs’ predicted property values (*x*-axis) and labels (*y*-axis) also differ (blobs). Before the costly step of acquiring design labels, design algorithm selection aims to choose design algorithm configurations that will satisfy a success criterion—for example, that the average design label surpasses a threshold (horizontal black line). This is challenging because designs’ predictions can be misleading; true labels can be low even if predictions are high (*e.g.*, rightmost blob). Our solution surmounts this by using held-out labeled data to characterize and remove the influence of prediction error in assessing the distributions of design labels, enabling trustworthy selection of configurations that satisfy the success criteria (green check marks).

guarantees on the selected configurations. First, we formalize design algorithm selection as a multiple hypothesis testing problem. We consider a finite set of candidate design algorithm configurations, called the *menu*, which we describe shortly. Each configuration on the menu is affiliated with a hypothesis test of whether it satisfies the success criterion. The method then computes a statistically valid p-value for this hypothesis test, by combining held-out labeled data with predicted property values for designs generated by the configuration. Loosely speaking, it uses the labeled data to characterize how prediction error biases a p-value based on predictions alone and removes this bias, building upon techniques from prediction-powered inference [2]. Finally, the p-values are assessed with a multiple testing correction to choose a set of design algorithm configurations. The method is guaranteed with high probability to select successful configurations (or return the null set if none are found), if the ratios between the design and labeled data densities are known for all configurations on the menu. If these density ratios are unknown, we show empirically that the method still frequently selects successful configurations using estimated density ratios.

The contents of the menu will depend on the task at hand. If a bespoke design algorithm has been developed specifically for the task, we may be interested in setting a key hyperparameter, such as real-valued hyperparameters that dictate how close to stay to the training data or other trusted points [36, 27, 7, 21, 16, 45]. The menu would then be a finite set of candidate values for that hyperparameter, such as a grid of values between plausible upper and lower bounds. In other cases, such as when a variety of design algorithms are appropriate for the task, we may want to consider multiple options for the design algorithm, its hyperparameter(s), and the predictive model it consults. The menu could then comprise all combinations of such options. Indeed, the menu can include or exclude any configuration we desire; we can include options for any degree of freedom whose effect on the designs we want to consider, while holding fixed those that can be reliably set by domain expertise.

Our contributions are as follows. We introduce the problem of design algorithm selection, which formalizes a consequential decision faced by practitioners of machine learning-guided design and links it to the goal of producing a distribution of design labels that satisfies a criterion. We propose a method for design algorithm selection, which combines designs’ predicted property values with held-out labeled data in a principled way to reliably assess whether candidate design algorithm configurations will be successful. We provide theoretical guarantees for the configurations selected by the method, if the ratios between the design and labeled data

densities are known. Finally, we demonstrate the method’s effectiveness on simulated protein and RNA design tasks, including settings where these density ratios are unknown and must be estimated.

2 Formalizing the design algorithm selection problem

This section formalizes the design algorithm selection problem. The next section proposes our solution.

The goal of a design task is to find novel objects in some domain, \mathcal{X} , whose labels in some space \mathcal{Y} satisfy a desired criterion. For example, one may seek protein sequences of length L , $x \in \mathcal{X} = \mathcal{A}^L$ where \mathcal{A} is the set of amino acids, whose real-valued catalytic activities for a reaction of interest, $y \in \mathcal{Y} = \mathbb{R}$, surpass some threshold. Note that it is often neither necessary nor feasible for every proposed design to satisfy the criterion—it is sufficiently useful that some of them do so. This observation guides our formalization of the *success criterion*, which we describe shortly. We first describe the other components of our framework.

Design algorithms are methods that output novel objects whose labels are believed to satisfy the desired criterion. We focus on those that consult a predictive model, though our framework is agnostic as to how they do so; they may also use other sources of information, such as unlabeled data or biomolecular structures. An example of a design algorithm for the aforementioned enzyme design task is to sample from a generative model fit to sequences that are evolutionarily related to a known enzyme, and return the samples with desirable predictions [46].

A **design algorithm configuration** or **configuration** is a specification of all the hyperparameter settings and models needed to deploy a design algorithm. Given a design task, a practitioner constructs a **menu**, Λ : a set of candidate configurations to be considered. For each configuration on the menu, $\lambda \in \Lambda$, we get predicted property values for N designs produced by the configuration: $\{f_\lambda(x_i^\lambda)\}_{i=1}^N$, where f_λ is the predictive model used by configuration λ .

We assume access to a set of i.i.d. **labeled data**: $x_i \sim P_{\text{lab}}, y_i \sim P_{Y|X=x}, i = 1, \dots, n$, where P_{lab} is the *labeled distribution* and $P_{Y|X=x}$ is the conditional distribution of the label random variable, Y , given the point x . We assume that this conditional distribution is fixed for every point in \mathcal{X} , as is the case when the label is dictated by the laws of nature. This data must be independent from the training data for the predictive models used on the menu, but it need not be from the training data distribution. Whenever unclear from context, we will say *held-out* or *additional* labeled data to disambiguate this data from the training data.

2.1 The success criterion

Given the above components, the goal of design algorithm selection is to select a subset of configurations, $\hat{\Lambda} \subseteq \Lambda$, that satisfy the *success criterion*, which we now formalize.

The designs produced by any design algorithm configuration, $\lambda \in \Lambda$, are sampled from some *design distribution* over \mathcal{X} , denoted $P_{X;\lambda}$. This distribution may be specified explicitly [8, 54], or only implicitly, such as when the algorithm iteratively introduces mutations to training sequences based on the resulting predicted property values [40]. The design distribution in turn induces the *design label distribution* over \mathcal{Y} , denoted $P_{Y;\lambda}$, which is the distribution of labels of designs drawn from $P_{X;\lambda}$ and can be sampled from as follows: $x \sim P_{X;\lambda}, y \sim P_{Y|X=x}$. Note that the labeled data and design data are related by covariate shift [38]: the distributions over \mathcal{X} differ, but the conditional distribution of the label given any point is fixed.

As previously noted, the aspiration for most design efforts in practice is not that every single design satisfies a criterion, but that enough of them do so [52]. Accordingly, our framework defines success in terms of the design label distribution, $P_{Y;\lambda}$, rather than the label of any specific design. The practitioner can specify any *success criterion* that can be expressed as the expected value of some function of the design labels surpassing some threshold:

$$\theta_\lambda := \mathbb{E}_{Y \sim P_{Y;\lambda}}[g(Y)] \geq \tau \tag{1}$$

for some $g : \mathcal{Y} \rightarrow \mathbb{R}$ and $\tau \in \mathbb{R}$.¹ Examples of this expected function value include the mean design label when g is the identity, as well as the fraction of designs whose labels exceed some value $\gamma \in \mathcal{Y}$, when $g(y) = \mathbb{1}[y \geq \gamma]$. Using the latter, for example, a practitioner can request that at least 10% of the designs’

¹See Appendix B.1 for generalization to other success criteria; here we focus on this special case for its broad applicability.

labels exceed that of a wild-type sequence, y_{WT} , using the success criterion $\mathbb{E}_{Y \sim P_{Y;\lambda}}[\mathbb{1}[Y \geq y_{\text{WT}}]] \geq 0.1$. We call a configuration *successful* if it yields a design label distribution that achieves the success criterion.

Our proposed method aims to select a subset of configurations from the menu such that, with guaranteed probability, every selected configuration is successful (or it returns the empty set, if no successful configuration exists on the menu). That is, for any user-specified error rate, $\alpha \in [0, 1]$, the goal is to construct a subset $\hat{\Lambda} \subseteq \Lambda$ such that

$$\mathbb{P}(\theta_\lambda \geq \tau, \forall \lambda \in \hat{\Lambda}) \geq 1 - \alpha. \quad (2)$$

If the density ratios between the design and labeled distributions are known for all configurations on the menu, our proposed method, which we detail next, guarantees Eq. 2.

3 Design algorithm selection by multiple hypothesis testing

Our method tackles design algorithm selection by approaching it as a multiple hypothesis testing problem (Alg. 1). The goal is to select a subset of configurations that are all successful, such that the *error rate*—the probability of incorrectly including one or more unsuccessful configurations—is at most α . To accomplish this, for each configuration on the menu consider the null hypothesis that it is unsuccessful: $H_\lambda : \theta_\lambda := \mathbb{E}_{Y \sim P_{Y;\lambda}}[g(Y)] < \tau$. We compute a p-value, p_λ , for testing against this null hypothesis, as we describe shortly. Finally, we use the Bonferroni correction to select all configurations whose p-values are sufficiently small. This subset of configurations satisfies Eq. 2, our goal for design algorithm selection.

Algorithm 1 Design algorithm selection by multiple hypothesis testing

Inputs: N designs generated by each design algorithm configuration on the menu, $\{x_i^\lambda\}_{i=1}^N, \forall \lambda \in \Lambda$; predictive models used by each configuration, $\{f_\lambda\}_{\lambda \in \Lambda}$; labeled data, $\{(x_i, y_i)\}_{i=1}^n$; error rate, $\alpha \in [0, 1]$.

Output: Selected configurations, $\hat{\Lambda} \subseteq \Lambda$.

```

1: for  $\lambda \in \Lambda$  do
2:    $\hat{y}_i^\lambda \leftarrow f_\lambda(x_i^\lambda), i \in [N]$ . ▷ Get predictions for designs
3:    $\hat{y}_j \leftarrow f_\lambda(x_j), j \in [n]$ . ▷ Get predictions for labeled data
4:    $p_\lambda \leftarrow \text{GETPVALUE}(\{\hat{y}_i^\lambda\}_{i=1}^N, \{(x_j, y_j, \hat{y}_j)\}_{j=1}^n)$ 
5: end for
6:  $\hat{\Lambda} \leftarrow \{\lambda \in \Lambda : p_\lambda \leq \alpha/|\Lambda|\}$ 

```

The key subproblem is obtaining statistically valid p-values for testing against the null hypotheses $H_\lambda, \lambda \in \Lambda$. These hypotheses concern expectations over the design label distributions, yet we do not have labels for the designs, only predictions. To extract information from these predictions without being misled by prediction error, we turn to prediction-powered inference [2], a framework that combines predictions with held-out labeled data to conduct valid statistical inference. Specifically, we use prediction-powered inference techniques adapted for covariate shift, due to the covariate-shift relationship between the design data and labeled data. We defer a thorough treatment to Appendix A, but conceptually, the labeled data, weighted by the density ratios between the design and labeled distributions, is used to characterize how prediction error distorts estimation of θ_λ based on predictions alone. This characterization of prediction error is then combined with the predictions for the designs to compute p-values that have either finite-sample (Alg. 3) or asymptotic (Alg. 2) validity. Using the former, the output of Algorithm 1 satisfies Eq. 2.

Theorem 1. *For any error rate, $\alpha \in [0, 1]$, function $g : \mathcal{Y} \rightarrow \mathbb{R}$, and threshold $\tau \in \mathbb{R}$, Algorithm 1 using Algorithm 3 as the p-value subroutine returns a subset of configurations from the menu, $\hat{\Lambda} \subseteq \Lambda$, that satisfies*

$$\mathbb{P}(\theta_\lambda \geq \tau, \forall \lambda \in \hat{\Lambda}) \geq 1 - \alpha$$

where $\theta_\lambda := \mathbb{E}_{Y \sim P_{Y;\lambda}}[g(Y)]$, and the probability is over random draws of the labeled data and the designs for all configurations on the menu.

Using asymptotically valid p-values (Alg. 2) yields an asymptotic version of the guarantee (Thm. 2). In experiments with known density ratios between the design and labeled distributions, we always achieved error rates under α even with asymptotically valid p-values. Since these are faster to compute, as they leverage closed-form expressions of the asymptotic null distributions, we recommend using these in practice.

Algorithm 2 Prediction-powered p-value for testing $H_\lambda : \theta_\lambda := \mathbb{E}_{Y \sim P_{Y;\lambda}}[g(Y)] < \tau$

Inputs: Predictions for designs, $\{\hat{y}'_i\}_{i=1}^N$; labeled data and their predictions, $\{(x_j, y_j, \hat{y}_j)\}_{j=1}^n$.

Output: p-value, P .

- 1: $\hat{\mu}_{\hat{y}'_i} \leftarrow \frac{1}{N} \sum_{i=1}^N g(\hat{y}'_i)$
 - 2: $w_j \leftarrow \text{DENSITYRATIO}(x_j), j = 1, \dots, n$ $\triangleright \text{DENSITYRATIO}(\cdot) := p_{X;\lambda}(\cdot)/p_{\text{train}}(\cdot)$
 - 3: $\hat{\Delta} \leftarrow \frac{1}{n} \sum_{j=1}^n w_j (g(y_j) - g(\hat{y}_j))$
 - 4: $\hat{\theta} \leftarrow \hat{\mu}_{\hat{y}'_i} + \hat{\Delta}$
 - 5: $\hat{\sigma}_{\hat{y}'_i}^2 \leftarrow \frac{1}{N} \sum_{i=1}^N (g(\hat{y}'_i) - \hat{\mu}_{\hat{y}'_i})^2$
 - 6: $\hat{\sigma}_{\hat{y}-y}^2 \leftarrow \frac{1}{n} \sum_{j=1}^n \left(w_j [g(y_j) - g(\hat{y}_j)] - \hat{\Delta} \right)^2$
 - 7: $P \leftarrow 1 - \Phi \left(\frac{(\hat{\theta} - \tau)}{\sqrt{\frac{\hat{\sigma}_{\hat{y}'_i}^2}{N} + \frac{\hat{\sigma}_{\hat{y}-y}^2}{n}}} \right)$ $\triangleright \Phi$ is the standard normal CDF
-

Selecting zero or multiple configurations Note that an error rate of zero can be trivially achieved by returning the empty set—that is, by never selecting any configuration. This is a legitimate outcome if there are no successful configurations on the menu, but otherwise, we will show empirically that our method also exhibits a high *selection rate* of returning nonempty sets. On the other hand, if our method selects multiple configurations then one can safely use any (or any mixture) of them with the same high-probability guarantee of achieving the success criterion. In particular, one can further narrow down $\hat{\Lambda}$ using additional criteria—for example, picking the selected configuration that produces the most diverse designs, in order to hedge against unknown future desiderata.

Density ratios between design and labeled distributions Computing the p-values requires the density ratio between the design and labeled distributions, $p_{X;\lambda}(x_i)/p_{\text{lab}}(x_i)$, for every configuration and every labeled instance. Important settings in biological sequence design where the design density can be evaluated are when designs are sampled from autoregressive generative models [39] or when the design distribution is a product of independent categorical distributions per sequence site, as in library design [51, 54]. Labeled sequence data is often generated by adding random substitutions to wild type sequences [7, 10] or by recombining segments of several “parent” sequences [33, 4], in which case p_{lab} is also explicitly known. Valid p-values can also be computed if both $p_{X;\lambda}$ and p_{lab} are only known up to normalizing factors, such as when sequences are generated by Potts models [34, 16] (Appendix B.2). In other settings, however, these density ratios need to be approximated. In experiments with unknown density ratios, we use multinomial logistic regression-based density ratio estimation [44] and show that our method still empirically outperforms others in selecting successful configurations. Although Theorems 1 or 2 no longer apply in this setting, they inform us what guarantees we can recover, to the extent that the density ratios are approximated well.

What does it mean to go “too far?” For any given configuration, $\lambda \in \Lambda$, the further apart the design and labeled distributions are, the higher the variance of the density ratios that are used to weight the labeled data. This reduces the effective sample size of the labeled data in characterizing prediction error, which leads to higher uncertainty about the value of θ_λ . Consequently, even if the configuration is successful, it may not be selected if the design and labeled distributions are too far apart. Indeed, this is desirable behavior: the method essentially identifies where over \mathcal{X} we lack sufficient statistical evidence of achieving the success criterion. It returns the empty set if the predictions and labeled data do not collectively provide adequate evidence that any configuration on the menu is successful.

4 Related work

Design algorithm selection belongs to a body of work on managing predictive uncertainty in machine learning-guided design. Design algorithms can be constrained to stay close to the training data or trusted reference points, such that predictions remain trustworthy [8, 27, 7, 21, 45], and out-of-distribution detection methods can be used to flag individual designs whose predictions are unreliable [12]. A variety of methods have been used to quantify predictive uncertainty for individual designs in biomolecular design tasks [19], including those based on ensembling [35, 20], Gaussian processes [23, 48], and evidential learning [41]. In particular, conformal prediction techniques construct prediction sets for designs that also have frequentist-style guarantees: the sets contain the design labels with guaranteed probability, where the probability is over drawing designs from the design distribution [15, 30]. However, it is unclear how to invoke such statements to make decisions about which designs to use, as there is no guarantee regarding the prediction sets for any *specific* designs of interest—for example, those whose prediction sets satisfy a desired condition.

Moreover, quantifying uncertainty for individual designs is perhaps unnecessary for the goal of many design campaigns in practice. Success often does not necessitate that every design performs as desired, but only that sufficiently many do so, regardless of which specific ones [52]. For example, Wang et al. [49] develop a method that selects designs from a pool of individual candidates, such that the selected subset contains a desired expected number whose label surpasses a threshold. However, the method requires held-out labeled data from the same distribution as the candidates, which is not always available in practice.

Conformal selection methods [24, 25, 3] combine ideas from conformal prediction and multiple testing to also select designs from a candidate pool, with guaranteed upper bounds on the false discovery rate, or expected proportion of selected designs whose label does not surpass a desired threshold. The setting of these methods differs from ours in that they assume access to a pool of candidates that are exchangeable—for example, candidates drawn i.i.d. from some distribution. However, depending on the application, it may not always be straightforward to narrow down a large design space \mathcal{X} to a suitable pool of candidates to begin with, without selecting a design algorithm configuration with which to generate designs. The goal of our work is therefore to choose from a set of candidate design algorithm configurations, each of which will produce a different distribution of designs when deployed. Our approach aims to select configurations that will achieve a population-level notion of success, which we formalize as a user-specified functional of the distribution of design labels, θ_λ , surpassing some threshold. Examples of this functional include the mean design label and the exceedance, or the fraction of design labels that exceed a threshold, and more generally any population-level quantity that can be expressed as minimizer of a convex loss (Appendix B.1).

Bayesian optimization (BO) [37] is a well-studied paradigm for iteratively selecting designs, acquiring their labels, and updating a predictive model in order to optimize a property of interest. In each round, in the language of our framework, BO prescribes a design algorithm: it chooses the design (or, more similar to our setting, the batch of designs [13]) that globally maximizes some *acquisition function* that quantifies desirability based on the model’s predictions, and which typically incorporates the model’s predictive uncertainty, such as the expected improvement of a design’s label over the best one found thus far. A typical goal of BO algorithms is to converge to the global optimum as the rounds progress indefinitely, under various regularity conditions on the property one seeks to optimize [43, 11, 5]. In contrast, the goal of design algorithm selection is to achieve guarantees on the distribution of design labels to be imminently proposed. Such guarantees are particularly useful and can help justify designs to stakeholders when acquiring labels for even one round is time- or resource-intensive, and the priority is to find designs that achieve specific improvements within one or a few rounds, rather than to eventually find the best possible design as the number of rounds goes to infinity. However, nothing precludes batch BO algorithms from being used as design algorithms within our framework if one deems them promising for the design task at hand. Configurations of batch BO algorithms with different hyperparameter settings or acquisition functions, for example, can be included on the menu alongside any other design algorithm configuration under consideration.

Similar to our work, Wheelock et al. [52] also focus on characterizing the design label distribution. After constructing a *forecast*, or model of the conditional distribution of the label, for every design, their approach uses an equally weighted mixture of designs’ forecasts as a model of the design label distribution. A rich body of work also exists on *calibrating* forecasts, such that various aspects of these conditional distributions are statistically consistent with held-out labeled data [17, 26, 42]. Our approach differs in that it directly estimates the functional of the design label distribution, θ_λ , that determines whether a configuration is

successful, rather than characterizing predictive uncertainty for individual designs. That is, our method handles prediction error in a way that is specifically tailored for the endpoint of selecting which design algorithm configuration to deploy.

At a technical level, our work uses prediction-powered inference techniques [2] adapted for covariate shift [38], in order to conduct statistically valid hypothesis tests of whether configurations are successful. The multiple hypothesis testing approach is similar to that of Angelopoulos et al. [1], who use multiple testing to select hyperparameter settings for predictive models in order to achieve desired risk values with high-probability guarantees.

5 Experiments

We first demonstrate that our method selects successful configurations with high probability, as guaranteed by theory, when the design and labeled densities are known. Next, we show that it still selects successful configurations more effectively than alternative methods when these densities are estimated.

Two metrics are of interest: error rate and selection rate. Error rate is the empirical frequency at which a method incorrectly selects a configuration that fails the success criterion (Eq. 1), computed over multiple trials of sampling designs from each configuration as well as held-out labeled data (for methods that require it). Selection rate is the empirical frequency over those same trials at which a method selects anything at all. A good method achieves a low error rate while maintaining a high selection rate, which may be challenging for ambitious success criteria.

For a fair comparison, we allowed the prediction-only and `GMMForecasts` methods, which do not use held-out labeled data, to use predictive models fit to the total amount of labeled data used by our method (i.e., the combination of 5k training and 5k held-out labeled instances).

Prediction-only method This baseline uses only the predictions for a configuration’s designs to assess whether it is successful. Specifically, it follows the same multiple testing framework as our method, but computes the p-values using the designs’ predictions as if they were labels (Alg. 6).

Gaussian-mixture-model forecast method For any sequence, Wheelock et al. [52] model the conditional distribution of the label as a mixture of two Gaussians with sequence-specific parameters, which capture beliefs over the label if the sequence is “functional” or “nonfunctional.” After training this model, they infer forecasts for every design produced by a configuration λ , where a hyperparameter $q \in [0, 1]$ controls, roughly speaking, how much the forecasts deviate from the training data (see Appendix C.2 for details). The equally weighted mixture of these forecasts serves as a model, P_λ^{GMM} , of the design label distribution for configuration λ . We select configurations using the following procedure, called `GMMForecasts`: for each $\lambda \in \Lambda$, we select λ if $\mathbb{E}_{Y \sim P_\lambda^{\text{GMM}}}[g(Y)] \geq \tau$.

Calibrated forecast method This method similarly models the design label distribution as the equally weighted mixture of forecasts for the designs produced by a configuration. Each forecast is initially modeled as a Gaussian with mean and variance set to the predictive mean and variance, respectively, given by the predictive model. We then use the labeled data to *calibrate* these forecasts *post hoc* using isotonic regression [26] (see Appendix C.3 for details). We select configuration λ if $\mathbb{E}_{Y \sim P_\lambda^{\text{cal}}}[g(Y)] \geq \tau$, where P_λ^{cal} is the equally weighted mixture of the calibrated forecasts for the designs. This procedure is called `CalibratedForecasts`.

Conformal prediction method We adapted conformal prediction techniques to conduct design algorithm selection, as detailed in Appendix C.4. This method has similar theoretical guarantees as our method, but is prohibitively conservative: across all our experiments, it achieved an error rate of zero by never selecting anything. We therefore exclude these results for clarity of visualization in Figures 3, 4, and 6.

5.1 Algorithm selection for designing protein GB1

The design task for the first set of experiments was to design novel protein sequences that have high binding affinity to an immunoglobulin, by specifying the amino acids at four particular sites of a protein called GB1.

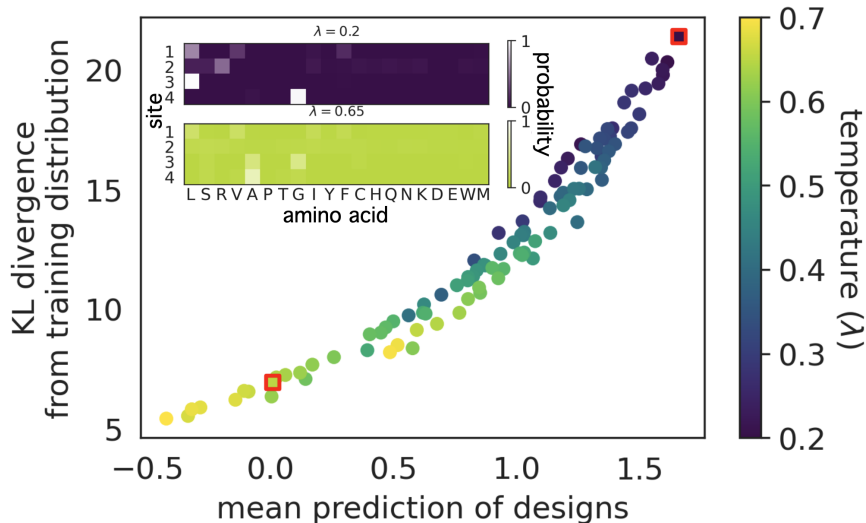


Figure 2: **Library design for protein GB1.** Mean prediction and KL divergence from the training distribution of the 101 design algorithm configurations on the menu. Each dot corresponds to the design distribution, q_λ , for a specific value of the temperature hyperparameter, λ . Two red-outlined squares correspond to design distributions for a low temperature ($\lambda = 0.2$) and a high temperature ($\lambda = 0.65$), whose parameters are shown in the insets (purple and green heatmaps, respectively).

These experiments simulate library design, an important practical setting in which both the design and labeled densities have closed-form expressions. Specifically, the most time- and cost-effective protocols today for synthesizing protein sequences in the wet lab can be described mathematically as sampling the amino acid at each site independently from a site-specific categorical distribution, whose parameters we can set; the density for any sequence is then the product of the probabilities of the amino acid at each site. We follow the design algorithm developed by Zhu, Brookes, & Busia *et al.* (2024): we first train a predictive model of binding affinity (Appendix D), f , and then set the parameters of the site-specific categorical distributions such that sequences with high predictions have high likelihood, as follows.

Let \mathcal{Q} denote the class of distributions that are products of four independent categorical distributions over twenty amino acids. The authors use stochastic gradient descent to approximately solve $q_\lambda = \arg \min_{q \in \mathcal{Q}} D_{\text{KL}}(p_\lambda^* \parallel q)$, where $p_\lambda^*(x) \propto \exp(f(x)/\lambda)$ and $\lambda > 0$ is a temperature hyperparameter that needs to be set carefully. Note that the training distribution, described shortly, was similar to a uniform distribution, which corresponds to $\lambda = \infty$. If λ is low, designs sampled from q_λ tend to have predictions that are high but untrustworthy since q_λ is far from the training distribution, while the opposite is true for high λ (Fig. 2). The goal is therefore to select λ such that q_λ is successful.

Labeled data To simulate training and held-out labeled data, we sampled sequences from a common baseline called the NNK library, which is close to uniform categorical distributions at every site, but slightly modified to reduce the probability of stop codons. For the labels, we used a data set that contains experimentally measured binding affinities for every sequence in \mathcal{X} [53]—that is, all 20^4 variants of protein GB1 at 4 specific sites. These labels were log-ratios relative to wild type GB1, such that the wild type’s label is 0.

Menu and success criteria The menu contained 101 values of λ between 0.2 and 0.7. We used the following success criteria: that the mean design label surpasses τ , for $\tau \in [0, 1.5]$ (for comparison, the mean training label was -4.8), and that the exceedance over 1 (i.e., the fraction of design labels that exceed 1) surpasses τ , for $\tau \in [0, 1]$ (for comparison, the training labels’ exceedance over 1 was 0.006).

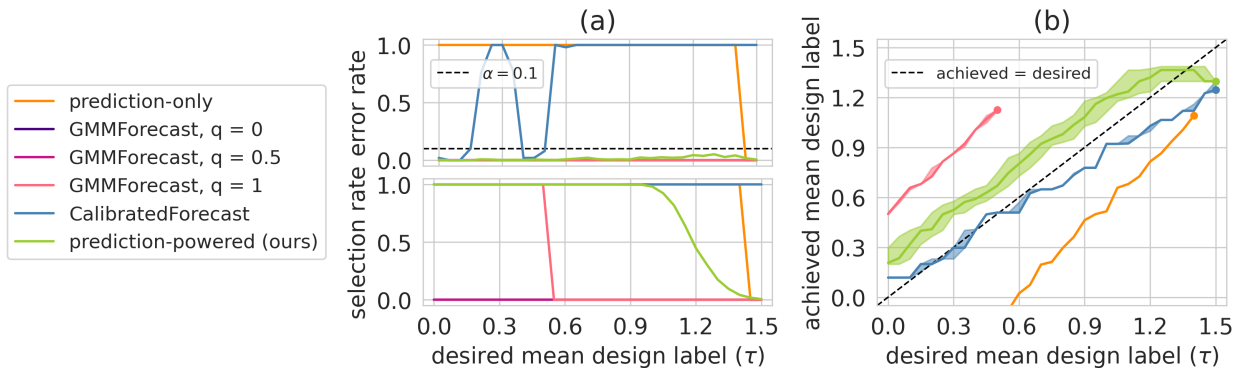


Figure 3: **Design algorithm selection for designing protein GB1.** (a) Error rate (top; lower is better) and selection rate (bottom; higher is better) for all methods, for range of values of τ , the desired mean design label. **GMMForecasts** with hyperparameter $q \in \{0, 0.5\}$ never selected anything, resulting in error and selection rates of zero for all τ . (b) For each method, the median (solid line) and 20th to 80th percentiles (shaded regions) of the lowest mean design label of selected configurations, over trials for the method did not return the empty set. Dots mark where each median trajectory ends (i.e., the value of τ beyond which a method ceases to select any configuration, and the mean design label achieved for that τ).

Selection experiments For the prediction-only method and **GMMForecasts**, which do not need held-out labeled data, we trained an ensemble of feedforward models on 10k labeled sequences. We then solved for q_λ , as described above, for all $\lambda \in \Lambda$. For each of $T = 10$ trials, we sampled $N = 1\text{M}$ designs from each q_λ and ran both methods to select temperatures.

For our method and **CalibratedForecasts**, which require held-out labeled data, we trained a feedforward ensemble on 5k labeled sequences and solved for $q_\lambda, \lambda \in \Lambda$. For each of $T = 500$ trials, we sampled $n = 5\text{k}$ additional labeled sequences, which were used to run both methods along with $N = 1\text{M}$ designs sampled from each q_λ .

For any $\lambda \in \Lambda$, the true value of θ_λ has a closed-form expression, since we have labels for all sequences in \mathcal{X} [53]. We then computed the error rate for each method as $\sum_{t=1}^T \mathbb{1}[\exists \lambda \in \hat{\Lambda} \text{ s.t. } \theta_\lambda < \tau] / T$. We used $\alpha = 0.1$ as a representative value for the desired error rate.

Results The prediction-only and **CalibratedForecasts** methods had error rates of 100% for most values of τ (Fig. 3a). Furthermore, particularly for the former, the true mean design label produced with selected temperatures could be considerably lower than τ (Fig. 3b).

Our method’s error rate was below α for all values of τ (Fig. 3a). That is, with frequency at least $1 - \alpha$, our method selected temperatures resulting in mean design labels that surpassed τ (Fig. 3b). The selection rate was also 100% for many values of τ , though it gradually declined for $\tau > 1$.

For **GMMForecasts**, note that smaller values of the hyperparameter $q \in [0, 1]$ yield forecasts that are, roughly speaking, more similar to the training data. Using $q \in \{0, 0.5\}$ was prohibitively conservative and never selected anything on any trial. Using the maximum value, $q = 1$, did result in high selection rates, but only for $\tau < 0.5$ (Fig. 3a). That is, if a more ambitious mean label was requested, the method incorrectly reported that no temperature could achieve it.

5.2 Algorithm selection for designing RNA binders

These next experiments show the utility of our method in a setting that involves a variety of design algorithms and predictive models on the menu, and that requires density ratio estimation. The task is to design length-50 RNA sequences that bind well to an RNA target, where the label is the ViennaFold binding energy [28].

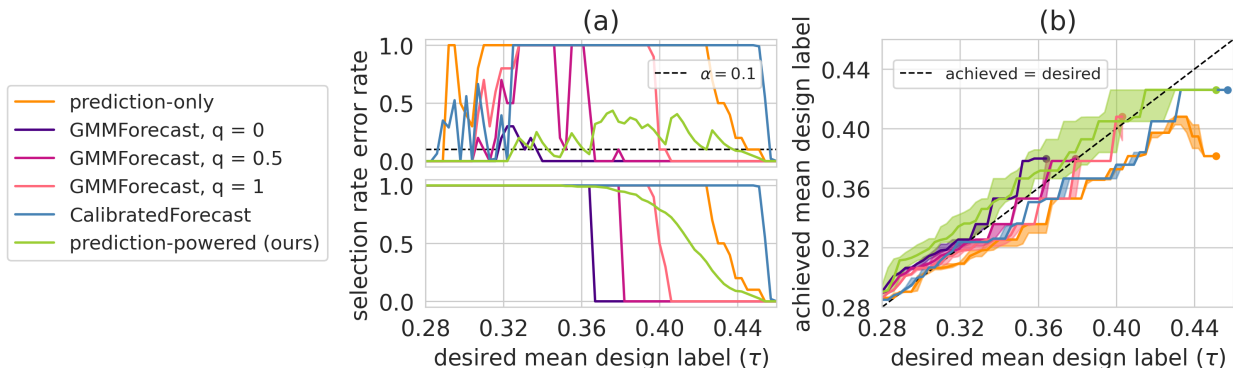


Figure 4: **Design algorithm selection for designing RNA binders.** (a) Error rate (top; lower is better) and selection rate (bottom; higher is better) for all methods, for range of values of τ , the desired mean design label. (b) For each method, the median (solid line) and 20th to 80th percentiles (shaded regions) of the lowest mean design label of selected configurations, over trials for the method did not return the empty set. Dots mark where each median trajectory ends (i.e., the value of τ beyond which a method ceases to select any configuration, and the mean design label achieved for that τ).

Labeled data To simulate training and held-out labeled data, we generated random mutants of a “seed” sequence, with 0.08 probability of mutation at each site. Each mutant, x , was given a noisy label, $y = \text{BINDINGENERGY}(x) + \epsilon$, where $\epsilon \sim \mathcal{N}(0, \sigma = 0.02)$.

Menu and success criteria The menu contains the following design algorithms and respective hyperparameter settings (see Appendix E.1 and Fig. 7 for details): **AdaLead** [40], with its threshold hyperparameter, κ , set to values in $[0.2, 0.01]$; the algorithm used by Biswas et al. [7], which approximately runs MCMC sampling from $p(x) \propto \exp(f(x)/T)$, where we set the temperature hyperparameter T to values in $[0.005, 0.02]$; Conditioning by Adaptive Sampling [8] and Design by Adaptive Sampling [9], with their quantile hyperparameter, Q , set to values in $[0.1, 0.9]$; and Proximal Exploration [31] with default hyperparameters, as the authors did not note any critical hyperparameters. Each of these design algorithms and respective hyperparameter settings was run with three different predictive models, resulting in a menu of 78 configurations: a ridge regression model, with the regularization hyperparameter set by leave-one-out cross-validation, an ensemble of feedforward neural networks, and an ensemble of convolutional neural networks. The selection criterion was that the mean design label surpasses τ , for $\tau \in [0.28, 0.5]$ (for comparison, the mean training label was 0.28).

Density ratio estimation None of the configurations have a closed-form design density. We therefore used multinomial logistic regression-based density ratio estimation (MDRE) [44], which trains a classifier between designs and labeled sequences to estimate the density ratios between their distributions (see Appendix E.2 for details).

Selection experiments For the prediction-only method and **GMMForecasts**, which do not require held-out labeled data, we first trained the three predictive models on 10k labeled sequences. For each of $T = 10$ trials, we sampled $N = 50\text{k}$ designs from each configuration and ran both methods to select configurations.

For our method and **CalibratedForecasts**, which use held-out labeled data, we trained the three predictive models on 5k labeled sequences. These sequences, as well as $N = 50\text{k}$ designs generated from each configuration, were used to fit the MDRE method. For each of $T = 200$ trials, we then sampled $n = 5\text{k}$ additional labeled sequences, which were used to run both methods along with the N designs from each configuration. Our method used the approximate density ratios provided by MDRE.

For each configuration, since there is no closed-form expression for θ_λ , we took the average of 500k design labels to serve as θ_λ . The error rate for each method was then computed as $\sum_{t=1}^T \mathbb{1}[\exists \lambda \in \hat{\Lambda} \text{ s.t. } \theta_\lambda < \tau]/T$, and we used $\alpha = 0.1$ as the desired error rate.

Results While our method’s error rate was not under α due to density ratio estimation error, it was much lower than those of the prediction-only and `CalibratedForecasts` methods, which had 100% error rates for most values of τ (Fig. 4a). Furthermore, when our method selected configurations that were unsuccessful, they still produced mean design labels close to τ (Fig. 4b). Our method assesses configurations more accurately at the cost of selections, $\hat{\Lambda}$, that are higher variance (Fig. 4b), due to the reduced effective sample size of the weighted labeled data.

`GMMForecasts` with $q = 0$ achieved low error rates, often even zero, for $\tau < 0.37$, but was very conservative: it stopped selecting configurations for greater τ (Fig. 4a). Using $q \in \{0.5, 1\}$ increased selection rates at the cost of much higher error rates, though, similar to our method, the effects of the errors were not severe for $q = 0.5$: the mean design labels of unsuccessful configurations were not far below τ (Fig. 4b).

6 Discussion

We introduced an algorithm selection method for machine learning-guided design, which selects design algorithm configurations that will be successful with high probability—that is, produce a distribution of design labels that satisfies a user-specified success criterion. It does so by using held-out labeled data to characterize and then undo how prediction error biases the assessment of whether a configuration is successful. Though the present work focuses on success in a single “round” of design, it can also provide a principled decision-making framework for multi-round design efforts in which a top priority is that the designs at each round achieve certain criteria—for example, to justify resources for acquiring their labels.

As with other uncertainty quantification methods that achieve frequentist-style guarantees under covariate shift [47, 15, 30, 25], the method uses the density ratios between the design and labeled distributions. Advances in density ratio estimation techniques will strengthen the method’s performance in settings where these density ratios are not known—in particular, techniques that are optimized specifically for importance-weighted mean estimation. Looking forward, we encourage continued work on how to address predictive uncertainty in machine learning-guided design with respect to how it directly impacts endpoints or decisions of interest, rather than with general-purpose notions of uncertainty [19].

7 Acknowledgments

Our gratitude goes to Anastasios N. Angelopoulos, Stephen Bates, Richard Bonneau, Andreas Loukas, Ewa Nowara, Stephen Ra, Samuel Stanton, Nataša Tagasovska, and Tijana Zrnic for helpful discussions and feedback on this work.

References

- [1] Anastasios N Angelopoulos, Stephen Bates, Emmanuel J Candès, Michael I Jordan, and Lihua Lei. Learn then test: Calibrating predictive algorithms to achieve risk control. *arXiv [cs.LG]*, October 2021.
- [2] Anastasios N Angelopoulos, Stephen Bates, Clara Fannjiang, Michael I Jordan, and Tijana Zrnic. Prediction-powered inference. *Science*, 382(6671):669–674, November 2023.
- [3] Tian Bai and Ying Jin. Optimized conformal selection: Powerful selective inference after conformity score optimization. *arXiv [stat.ME]*, November 2024.
- [4] Claire N Bedbrook, Kevin K Yang, J Elliott Robinson, Elisha D Mackey, Viviana Gradinaru, and Frances H Arnold. Machine learning-guided channelrhodopsin engineering enables minimally invasive optogenetics. *Nat. Methods*, 16(11):1176–1184, November 2019.

- [5] Felix Berkenkamp, Angela P Schoellig, and Andreas Krause. No-regret bayesian optimization with unknown hyperparameters. *J. Mach. Learn. Res.*, abs/1901.03357(50):1–24, January 2019.
- [6] S Bickel, M Bruckner, and T Scheffer. Discriminative learning under covariate shift. *J. Mach. Learn. Res.*, 10:2137–2155, 2009.
- [7] Surojit Biswas, Grigory Khimulya, Ethan C Alley, Kevin M Esvelt, and George M Church. Low-N protein engineering with data-efficient deep learning. *Nat. Methods*, 18(4):389–396, April 2021.
- [8] David Brookes, Hahnbeom Park, and Jennifer Listgarten. Conditioning by adaptive sampling for robust design. In Kamalika Chaudhuri and Ruslan Salakhutdinov, editors, *Proceedings of the 36th International Conference on Machine Learning*, volume 97 of *Proceedings of Machine Learning Research*, pages 773–782. PMLR, 09–15 Jun 2019. URL <https://proceedings.mlr.press/v97/brookes19a.html>.
- [9] David H Brookes and Jennifer Listgarten. Design by adaptive sampling. In *NeurIPS Workshop on Machine Learning for Molecules and Materials*, 2018.
- [10] Drew H Bryant, Ali Bashir, Sam Sinai, Nina K Jain, Pierce J Ogden, Patrick F Riley, George M Church, Lucy J Colwell, and Eric D Kelsic. Deep diversification of an AAV capsid protein by machine learning. *Nat. Biotechnol.*, February 2021.
- [11] Adam D. Bull. Convergence rates of efficient global optimization algorithms. *Journal of Machine Learning Research*, 12(88):2879–2904, 2011. URL <http://jmlr.org/papers/v12/bull11a.html>.
- [12] Farhan Damani, David H Brookes, Theodore Sternlieb, Cameron Webster, Stephen Malina, Rishi Jajoo, Kathy Lin, and Sam Sinai. Beyond the training set: an intuitive method for detecting distribution shift in model-based optimization. *arXiv [cs.LG]*, November 2023.
- [13] Thomas Desautels, Andreas Krause, and Joel W Burdick. Parallelizing exploration-exploitation tradeoffs in gaussian process bandit optimization. *J. Mach. Learn. Res.*, 15(1):3873–3923, 2014.
- [14] Clara Fannjiang and Jennifer Listgarten. Is novelty predictable? *Cold Spring Harb. Perspect. Biol.*, 16(2):a041469, February 2024.
- [15] Clara Fannjiang, Stephen Bates, Anastasios N Angelopoulos, Jennifer Listgarten, and Michael I Jordan. Conformal prediction under feedback covariate shift for biomolecular design. *Proc. Natl. Acad. Sci. U. S. A.*, 119(43):e2204569119, October 2022.
- [16] Benjamin Fram, Yang Su, Ian Truebridge, Adam J Riesselman, John B Ingraham, Alessandro Passera, Eve Napier, Nicole N Thadani, Samuel Lim, Kristen Roberts, Gurleen Kaur, Michael A Stiffler, Debora S Marks, Christopher D Bahl, Amir R Khan, Chris Sander, and Nicholas P Gauthier. Simultaneous enhancement of multiple functional properties using evolution-informed protein design. *Nat. Commun.*, 15(1):5141, June 2024.
- [17] Tilmann Gneiting, Fadoua Balabdaoui, and Adrian E Raftery. Probabilistic forecasts, calibration and sharpness. *J. R. Stat. Soc. Series B Stat. Methodol.*, 69(2):243–268, April 2007.
- [18] Jonathan C Greenhalgh, Sarah A Fahlberg, Brian F Pfeleger, and Philip A Romero. Machine learning-guided acyl-ACP reductase engineering for improved in vivo fatty alcohol production. *Nat. Commun.*, 12(1):5825, October 2021.
- [19] Kevin P Greenman, Ava P Amini, and Kevin K Yang. Benchmarking uncertainty quantification for protein engineering. *PLoS Comput. Biol.*, 21(1):e1012639, January 2025.
- [20] Nate Gruver, Samuel Stanton, Polina Kirichenko, Marc Finzi, Phillip Maffettone, Vivek Myers, Emily Delaney, Peyton Greenside, and Andrew Gordon Wilson. Effective Surrogate Models for Protein Design with Bayesian Optimization. In *ICML Workshop on Computational Biology*, 2021.

- [21] Nate Gruver, Samuel Stanton, Nathan Frey, Tim G. J. Rudner, Isidro Hotzel, Julien Lafrance-Vanasse, Arvind Rajpal, Kyunghyun Cho, and Andrew G Wilson. Protein design with guided discrete diffusion. In A. Oh, T. Naumann, A. Globerson, K. Saenko, M. Hardt, and S. Levine, editors, *Advances in Neural Information Processing Systems*, volume 36, pages 12489–12517. Curran Associates, Inc., 2023. URL https://proceedings.neurips.cc/paper_files/paper/2023/file/29591f355702c3f4436991335784b503-Paper-Conference.pdf.
- [22] Michael U Gutmann and Aapo Hyvärinen. Noise-contrastive estimation of unnormalized statistical models, with applications to natural image statistics. *J. Mach. Learn. Res.*, 13(11):307–361, 2012.
- [23] Brian Hie, Bryan D Bryson, and Bonnie Berger. Leveraging uncertainty in machine learning accelerates biological discovery and design. *Cell Syst*, 11(5):461–477.e9, November 2020.
- [24] Ying Jin and E Candès. Selection by prediction with conformal p-values. *J. Mach. Learn. Res.*, 24(244):244:1–244:41, October 2022.
- [25] Ying Jin and Emmanuel J Candès. Model-free selective inference under covariate shift via weighted conformal p-values. *arXiv [stat.ME]*, July 2023.
- [26] Volodymyr Kuleshov, Nathan Fenner, and Stefano Ermon. Accurate uncertainties for deep learning using calibrated regression. In Jennifer Dy and Andreas Krause, editors, *Proceedings of the 35th International Conference on Machine Learning*, volume 80 of *Proceedings of Machine Learning Research*, pages 2796–2804. PMLR, 10–15 Jul 2018.
- [27] Johannes Linder, Nicholas Bogard, Alexander B Rosenberg, and Georg Seelig. A generative neural network for maximizing fitness and diversity of synthetic DNA and protein sequences. *Cell Syst*, 11(1):49–62.e16, July 2020.
- [28] Ronny Lorenz, Stephan H Bernhart, Christian Höner Zu Siederdisen, Hakim Tafer, Christoph Flamm, Peter F Stadler, and Ivo L Hofacker. ViennaRNA package 2.0. *Algorithms Mol. Biol.*, 6:26, November 2011.
- [29] Art B. Owen. *Monte Carlo Theory, Methods, and Examples*. <https://artowen.su.domains/mc/>, 2013.
- [30] Drew Prinster, Suchi Saria, and Anqi Liu. JAWS-x: Addressing efficiency bottlenecks of conformal prediction under standard and feedback covariate shift. In Andreas Krause, Emma Brunskill, Kyunghyun Cho, Barbara Engelhardt, Sivan Sabato, and Jonathan Scarlett, editors, *Proceedings of the 40th International Conference on Machine Learning*, volume 202 of *Proceedings of Machine Learning Research*, pages 28167–28190. PMLR, 23–29 Jul 2023. URL <https://proceedings.mlr.press/v202/prinster23a.html>.
- [31] Zhizhou Ren, Jiahan Li, Fan Ding, Yuan Zhou, Jianzhu Ma, and Jian Peng. Proximal exploration for model-guided protein sequence design. In Kamalika Chaudhuri, Stefanie Jegelka, Le Song, Csaba Szepesvari, Gang Niu, and Sivan Sabato, editors, *Proceedings of the 39th International Conference on Machine Learning*, volume 162 of *Proceedings of Machine Learning Research*, pages 18520–18536. PMLR, 17–23 Jul 2022. URL <https://proceedings.mlr.press/v162/ren22a.html>.
- [32] Benjamin Rhodes, Kai Xu, and Michael U. Gutmann. Telescoping density-ratio estimation. In H. Larochelle, M. Ranzato, R. Hadsell, M.F. Balcan, and H. Lin, editors, *Advances in Neural Information Processing Systems*, volume 33, pages 4905–4916. Curran Associates, Inc., 2020. URL https://proceedings.neurips.cc/paper_files/paper/2020/file/33d3b157ddc0896addfb22fa2a519097-Paper.pdf.
- [33] Philip A Romero, Andreas Krause, and Frances H Arnold. Navigating the protein fitness landscape with gaussian processes. *Proc. Natl. Acad. Sci. U. S. A.*, 110(3):E193–201, January 2013.
- [34] William P Russ, Matteo Figliuzzi, Christian Stocker, Pierre Barrat-Charlaix, Michael Socolich, Peter Kast, Donald Hilvert, Remi Monasson, Simona Cocco, Martin Weigt, and Rama Ranganathan. An evolution-based model for designing chorismate mutase enzymes. *Science*, 369(6502):440–445, July 2020.

- [35] Gabriele Scalia, Colin A Grambow, Barbara Pernici, Yi-Pei Li, and William H Green. Evaluating scalable uncertainty estimation methods for deep learning-based molecular property prediction. *J. Chem. Inf. Model.*, 60(6):2697–2717, June 2020.
- [36] Benjamin Schubert, Charlotta Schärfe, Pierre Dönnès, Thomas Hopf, Debora Marks, and Oliver Kohlbacher. Population-specific design of de-immunized protein biotherapeutics. *PLoS Comput. Biol.*, 14(3):e1005983, March 2018.
- [37] Bobak Shahriari, Kevin Swersky, Ziyu Wang, Ryan P Adams, and Nando de Freitas. Taking the human out of the loop: A review of bayesian optimization. *Proc. IEEE*, 104(1):148–175, January 2016.
- [38] Hidetoshi Shimodaira. Improving predictive inference under covariate shift by weighting the log-likelihood function. *J. Stat. Plan. Inference*, 90(2):227–244, October 2000.
- [39] Jung-Eun Shin, Adam J Riesselman, Aaron W Kollasch, Conor McMahon, Elana Simon, Chris Sander, Aashish Manglik, Andrew C Kruse, and Debora S Marks. Protein design and variant prediction using autoregressive generative models. *Nat. Commun.*, 12(1):2403, April 2021.
- [40] Sam Sinai, Richard Wang, Alexander Whatley, Stewart Slocum, Elina Locane, and Eric D Kelsic. AdaLead: A simple and robust adaptive greedy search algorithm for sequence design. October 2020.
- [41] Ava P Soleimany, Alexander Amini, Samuel Goldman, Daniela Rus, Sangeeta N Bhatia, and Connor W Coley. Evidential deep learning for guided molecular property prediction and discovery. *ACS Cent Sci*, 7(8):1356–1367, August 2021.
- [42] Hao Song, Tom Diethe, Meelis Kull, and Peter Flach. Distribution calibration for regression. In Kamalika Chaudhuri and Ruslan Salakhutdinov, editors, *Proceedings of the 36th International Conference on Machine Learning*, volume 97 of *Proceedings of Machine Learning Research*, pages 5897–5906. PMLR, 09–15 Jun 2019.
- [43] Niranjan Srinivas, Andreas Krause, Sham Kakade, and Matthias Seeger. Gaussian process optimization in the bandit setting: no regret and experimental design. In *Proceedings of the 27th International Conference on International Conference on Machine Learning*, ICML’10, page 1015–1022, Madison, WI, USA, 2010. Omnipress. ISBN 9781605589077.
- [44] Akash Srivastava, Seungwook Han, Kai Xu, Benjamin Rhodes, and Michael U. Gutmann. Estimating the density ratio between distributions with high discrepancy using multinomial logistic regression. *Transactions on Machine Learning Research*, 2023. ISSN 2835-8856. URL <https://openreview.net/forum?id=jM8nzUzBWr>.
- [45] Nataša Tagasovska, Vladimir Gligorijević, Kyunghyun Cho, and Andreas Loukas. Implicitly guided design with PropEn: Match your data to follow the gradient. In *Advances in Neural Information Processing Systems*, volume 37, 2024.
- [46] Neil Thomas, David Belanger, Chenling Xu, Hanson Lee, Kathleen Hirano, Kosuke Iwai, Vanja Polic, Kendra D Nyberg, Kevin G Hoff, Lucas Frenz, Charlie A Emrich, Jun W Kim, Mariya Chavarha, Abi Ramanan, Jeremy J Agresti, and Lucy J Colwell. Engineering of highly active and diverse nuclease enzymes by combining machine learning and ultra-high-throughput screening. *bioRxiv*, page 2024.03.21.585615, March 2024.
- [47] Ryan J Tibshirani, Rina Foygel Barber, Emmanuel Candes, and Aaditya Ramdas. Conformal prediction under covariate shift. In *Advances in Neural Information Processing Systems*, volume 32, pages 2530–2540. 2019. URL <https://proceedings.neurips.cc/paper/2019/file/8fb21ee7a2207526da55a679f0332de2-Paper.pdf>.
- [48] Kevin Tran, Willie Neiswanger, Junwoong Yoon, Qingyang Zhang, Eric Xing, and Zachary W Ulissi. Methods for comparing uncertainty quantifications for material property predictions. *Mach. Learn. Sci. Technol.*, 1(2):025006, June 2020.

- [49] Lequn Wang, Thorsten Joachims, and Manuel Gomez Rodriguez. Improving screening processes via calibrated subset selection. In Kamalika Chaudhuri, Stefanie Jegelka, Le Song, Csaba Szepesvári, Gang Niu, and Sivan Sabato, editors, *International Conference on Machine Learning, ICML 2022, 17-23 July 2022, Baltimore, Maryland, USA*, volume 162 of *Proceedings of Machine Learning Research*, pages 22702–22726. PMLR, 2022. URL <https://proceedings.mlr.press/v162/wang22j.html>.
- [50] Ian Waudby-Smith and Aaditya Ramdas. Estimating means of bounded random variables by betting. *J. R. Stat. Soc. Series B Stat. Methodol.*, February 2023.
- [51] Eli N. Weinstein, Alan N. Amin, Will S. Grathwohl, Daniel Kassler, Jean Disset, and Debora Marks. Optimal design of stochastic dna synthesis protocols based on generative sequence models. In Gustau Camps-Valls, Francisco J. R. Ruiz, and Isabel Valera, editors, *Proceedings of The 25th International Conference on Artificial Intelligence and Statistics*, volume 151 of *Proceedings of Machine Learning Research*, pages 7450–7482. PMLR, 28–30 Mar 2022. URL <https://proceedings.mlr.press/v151/weinstein22a.html>.
- [52] Lauren B Wheelock, Stephen Malina, Jeffrey Gerold, and Sam Sinai. Forecasting labels under distribution-shift for machine-guided sequence design. In David A Knowles, Sara Mostafavi, and Su-In Lee, editors, *Proceedings of the 17th Machine Learning in Computational Biology Meeting*, volume 200 of *Proceedings of Machine Learning Research*, pages 166–180. PMLR, 2022.
- [53] Nicholas C Wu, Lei Dai, C Anders Olson, James O Lloyd-Smith, and Ren Sun. Adaptation in protein fitness landscapes is facilitated by indirect paths. *eLife*, 5, July 2016.
- [54] Danqing Zhu, David H Brookes, Akosua Busia, Ana Carneiro, Clara Fannjiang, Galina Popova, David Shin, Kevin C Donohue, Li F Lin, Zachary M Miller, Evan R Williams, Edward F Chang, Tomasz J Nowakowski, Jennifer Listgarten, and David V Schaffer. Optimal trade-off control in machine learning-based library design, with application to adeno-associated virus (AAV) for gene therapy. *Sci Adv*, 10 (4):eadj3786, January 2024.

Appendix

A Algorithms and proofs

Algorithm 3 Prediction-powered p-value for testing $H_\lambda : \theta_\lambda < \tau$ (finite sample-valid)

Inputs: Predictions for designs, $\{\hat{y}'_i\}_{i=1}^N$; labeled data and their predictions, $\{(x_j, y_j, \hat{y}_j)\}_{j=1}^n$; fine grid spacing, $\delta > 0$.

Output: p-value, P .

```

1:  $w_j \leftarrow \text{DENSITYRATIO}(x_j), j = 1, \dots, n$ 
2: for  $\alpha \in \{0, \delta, \dots, 1 - \delta, 1\}$  do
3:    $L_\alpha \leftarrow \text{PPMEANLB}(\alpha, \{\hat{y}'_i\}_{i=1}^N, \{(w_j, y_j, \hat{y}_j)\}_{j=1}^n)$ 
4:   if  $L_\alpha > \tau$  then
5:      $P \leftarrow \alpha$ 
6:   break
7: end if
8: end for

```

Algorithm 4 PPMEANLB: Prediction-powered confidence lower bound on $\theta_\lambda := \mathbb{E}_{Y \sim P_{Y;\lambda}}[g(Y)]$ (finite sample-valid)

Inputs: Significance level, $\alpha \in [0, 1]$; predictions for designs, $\{\hat{y}'_i\}_{i=1}^N$; labeled data and their density ratios and predictions, $\{(w_i, y_i, \hat{y}_i)\}_{i=1}^n$; range, $[L, U]$, of $g(Y)$; bound, B , on the density ratios.

Output: Confidence lower bound, L .

```

1:  $\hat{\mu}_{\text{lower}} \leftarrow \text{MEANLB}(0.1 \cdot \alpha, \{g(\hat{y}'_i)\}_{i=1}^N, [L, U])$ 
2:  $\Delta_{\text{lower}} \leftarrow \text{MEANLB}(0.9 \cdot \alpha, \{w_j \cdot (g(\hat{y}_j) - g(y_j))\}_{j=1}^n, [B(L - U), B(U - L)])$ 
3:  $L \leftarrow \hat{\mu}_{\text{lower}} + \Delta_{\text{lower}}$ 

```

Theorem 2. For any error rate, $\alpha \in [0, 1]$, function $g : \mathcal{Y} \rightarrow \mathbb{R}$, and threshold $\tau \in \mathbb{R}$, Algorithm 1 using Algorithm 2 as the p-value subroutine returns a subset of configurations from the menu, $\hat{\Lambda} \subseteq \Lambda$, that satisfies

$$\liminf_{n, N \rightarrow \infty} \mathbb{P}(\theta_\lambda \geq \tau, \forall \lambda \in \hat{\Lambda}) \geq 1 - \alpha, \quad (3)$$

where $\theta_\lambda \equiv \mathbb{E}_{Y \sim P_{Y;\lambda}}[g(Y)]$, n and N are the amounts of labeled data and designs sampled per configuration, respectively, $\frac{n}{N} \rightarrow r$ for some $r \in (0, 1)$, and the probability is over random draws of the labeled data and the designs for all configurations on the menu.

The proofs of Theorems 1 and 2 rely on establishing the validity of the p-values computed by Algorithms 3 and 2, respectively. Both algorithms use the framework of prediction-powered inference [2], which estimates a population-level estimand of interest—here, $\mathbb{E}_{Y \sim P_{Y;\lambda}}[g(Y)]$ —by combining predictions for Y with an estimand-specific characterization of prediction error called the *rectifier*. For our estimand, these two components emerge from the following simple decomposition:

$$\mathbb{E}_{Y \sim P_{Y;\lambda}}[g(Y)] = \mathbb{E}_{X \sim P_{X;\lambda}}[g(f(X))] + \mathbb{E}_{X, Y \sim P_{X;\lambda} \cdot P_{Y|X}}[g(Y) - g(f(X))], \quad (4)$$

where the first summand is the mean prediction for designs, and the second is the mean prediction bias, which serves as the rectifier. More generally, prediction-powered inference encompasses any estimand that can be expressed as the minimizer of an expected convex loss (see Appendix B.1), in which case the rectifier can be derived from a similar decomposition of that loss's gradient.

To estimate the two terms in Eq. 4, we can use the predictions for N designs to estimate the first, and the n labeled instances to estimate the second, the rectifier. In particular, since the rectifier is an expectation

Algorithm 5 MEANLB: Confidence lower bound on a mean (finite sample-valid; Waudby-Smith and Ramdas [50])

Inputs: Significance level, $\alpha \in [0, 1]$; data, $\{z_i\}_{i=1}^n$; range of random variable, $[L, U]$.

Output: Confidence lower bound, B .

```

1:  $z_i \leftarrow (z_i - L)/(U - L), i = 1, \dots, n$ 
2:  $\mathcal{A} \leftarrow \{0, \delta, \dots, 1 - \delta, 1\}$ 
3:  $M_0^+(m) \leftarrow 1, m \in \mathcal{A}$ 
4:  $M_0^-(m) \leftarrow 1, m \in \mathcal{A}$ 
5: for  $t = 1, \dots, n$  do
6:    $\hat{\mu}_t \leftarrow \frac{0.5 + \sum_{j=1}^t z_j}{t+1}, \hat{\sigma}_t^2 \leftarrow \frac{0.25 + \sum_{j=1}^t (z_j - \hat{\mu}_t)^2}{t+1}, \lambda_t \leftarrow \sqrt{\frac{2 \log(2/\alpha)}{n \hat{\sigma}_{t-1}^2}}$ 
7:   for  $m \in \mathcal{A}$  do
8:      $M_t^+(m) \leftarrow (1 + \min\{\lambda_t, \frac{0.5}{m}\}(z_t - m)) M_{t-1}^+(m)$ 
9:      $M_t^-(m) \leftarrow (1 - \min\{\lambda_t, \frac{0.5}{1-m}\}(z_t - m)) M_{t-1}^-(m)$ 
10:     $M_t(m) = 0.5 \cdot \max\{M_t^+(m), M_t^-(m)\}$ 
11:    if  $M_t(m) \geq 1/\alpha$  then
12:       $\mathcal{A} \leftarrow \mathcal{A} \setminus \{m\}$ 
13:    end if
14:  end for
15: end for
16:  $B \leftarrow \min \mathcal{A} \cdot (U - L) + L$ 

```

over designs and their labels, we leverage the covariate shift relationship between the distributions of the designs and the labeled data to rewrite it as

$$\begin{aligned} \mathbb{E}_{X, Y \sim P_{X, \lambda} \cdot P_{Y|X}}[g(Y) - g(f(X))] &= \mathbb{E}_{X, Y \sim P_{\text{lab}} \cdot P_{Y|X}} \left[\frac{p_{X; \lambda}(X) p_{Y|X}(Y | X)}{p_{\text{lab}}(X) p_{Y|X}(Y | X)} (g(Y) - g(f(X))) \right] \\ &= \mathbb{E}_{X, Y \sim P_{\text{lab}} \cdot P_{Y|X}} \left[\frac{p_{X; \lambda}(X)}{p_{\text{lab}}(X)} (g(Y) - g(f(X))) \right]. \end{aligned}$$

This last expression can be estimated using the labeled data, where each instance is weighted by the density ratio between the design and label distributions. Adding together the estimates of the two terms in Eq. 4 yields a prediction-powered estimate of $\mathbb{E}_{Y \sim P_{Y; \lambda}}[g(Y)]$, and a prediction-powered p-value can be computed based on this estimate. Specifically, Algorithm 2 follows standard protocol for constructing asymptotically valid p-values, by first deriving the asymptotic null distribution of this prediction-powered estimate, and then evaluating its survival function to produce a p-value. Algorithm 3 relies on inverting finite sample-valid, prediction-powered confidence lower bounds on $\mathbb{E}_{Y \sim P_{Y; \lambda}}[g(Y)]$ to obtain p-values.

We now briefly describe why the prediction-powered estimate of $\mathbb{E}_{Y \sim P_{Y; \lambda}}[g(Y)]$ is statistically more powerful—and yields correspondingly more powerful p-values—than ignoring the N predictions and using only the n weighted labeled instances to estimate it, rewritten as

$$\begin{aligned} \mathbb{E}_{Y \sim P_{Y; \lambda}}[g(Y)] &= \mathbb{E}_{X, Y \sim P_{X, \lambda} \cdot P_{Y|X}}[g(Y)] = \mathbb{E}_{X, Y \sim P_{\text{lab}} \cdot P_{Y|X}} \left[\frac{p_{X; \lambda}(X) p_{Y|X}(Y | X)}{p_{\text{lab}}(X) p_{Y|X}(Y | X)} g(Y) \right] \\ &= \mathbb{E}_{X, Y \sim P_{\text{lab}} \cdot P_{Y|X}} \left[\frac{p_{X; \lambda}(X)}{p_{\text{lab}}(X)} g(Y) \right]. \end{aligned} \quad (5)$$

Critically, we assume that $N \gg n$, as it is typically far cheaper to computationally generate designs than it is to acquire labeled data. For $N \gg n$, the variance of the estimate of the first term in Eq. 4 will be negligible compared to that of the rectifier; indeed, we can make it arbitrarily small by computationally generating more designs from a given configuration. The variance of the prediction-powered estimate is therefore dominated by the variance of the rectifier estimate using the n labeled instances. Furthermore, the rectifier will be small so long as the predictions carry some information about the labels, so the variance of its estimate will likely be well below that of an estimate of Eq. 5 using those same n labeled instances.

A.1 Proof of Theorem 2 (asymptotically valid design algorithm selection)

Proof. We first establish the asymptotic validity of the p-value, p_λ , computed by Algorithm 2. Specifically, we show that under the null hypothesis, $H_\lambda : \theta_\lambda < \tau$, p_λ is the survival function of the asymptotic distribution of the prediction-powered estimate $\hat{\theta}$, and therefore satisfies

$$\limsup_{n, N \rightarrow \infty} \mathbb{P}(p_\lambda \leq u) \leq u, \quad \forall u \in [0, 1], \quad (6)$$

where $n/N \rightarrow r$ for some $r \in (0, 1)$.

We first derive the asymptotic distribution of $\hat{\theta} = \hat{\mu}_{\hat{y}'} + \hat{\Delta}$, where $\hat{\mu}_{\hat{y}'} = (1/N) \sum_{i=1}^N g(\hat{y}'_i)$ is the average prediction for N designs, and $\hat{\Delta} = (1/n) \sum_{j=1}^n w_j (g(y_j) - g(\hat{y}_j))$ where $w_j = p_{X;\lambda}(x_j)/p_{\text{lab}}(x_j)$ is the importance-weighted average bias of predictions for the n labeled instances. The central limit theorem implies that

$$\begin{aligned} \sqrt{N}(\hat{\mu}_{\hat{y}'} - \mathbb{E}[\hat{\mu}_{\hat{y}'}]) &\xrightarrow{d} \mathcal{N}(0, \sigma_{\hat{y}'}^2), \\ \sqrt{n}(\hat{\Delta} - \mathbb{E}[\hat{\Delta}]) &\xrightarrow{d} \mathcal{N}(0, \sigma_{\hat{y}'-y'}^2), \end{aligned}$$

where $\sigma_{\hat{y}'}^2 = \text{Var}_{X \sim P_{X;\lambda}}[g(f(X))]$ and $\sigma_{\hat{y}'-y'}^2 = \text{Var}_{X, Y \sim P_{X;\lambda} \cdot P_{Y|X}}[g(Y) - g(f(X))]$. Since $\hat{\mu}_{\hat{y}'}$ and $\hat{\Delta}$ are independent, we can apply the continuous mapping theorem to their sum to get that

$$\begin{aligned} \sqrt{N}(\hat{\mu}_{\hat{y}'} + \hat{\Delta} - \mathbb{E}[\hat{\mu}_{\hat{y}'} + \hat{\Delta}]) &= \sqrt{N}(\hat{\mu}_{\hat{y}'} - \mathbb{E}[\hat{\mu}_{\hat{y}'}]) + \sqrt{\frac{N}{n}} \sqrt{n}(\hat{\Delta} - \mathbb{E}[\hat{\Delta}]) \\ &\xrightarrow{d} \mathcal{N}(0, \sigma_{\hat{y}'}^2 + \frac{1}{r} \sigma_{\hat{y}'-y'}^2) \end{aligned}$$

where recall $n/N \rightarrow r$. Since

$$\mathbb{E}[\hat{\mu}_{\hat{y}'} + \hat{\Delta}] = \mathbb{E}_{X \sim P_{X;\lambda}}[g(f(X))] + \mathbb{E}_{X, Y \sim P_{X;\lambda} \cdot P_{Y|X}}[g(Y) - g(f(X))] = \mathbb{E}_{Y \sim P_{Y;\lambda}}[g(Y)] := \theta_\lambda,$$

we equivalently have

$$\sqrt{N}(\hat{\mu}_{\hat{y}'} + \hat{\Delta} - \theta_\lambda) \xrightarrow{d} \mathcal{N}(0, \sigma_{\hat{y}'}^2 + \frac{1}{r} \sigma_{\hat{y}'-y'}^2).$$

We can now evaluate the survival function of this distribution under the null hypothesis, $H_\lambda : \theta_\lambda < \tau$, to obtain a p-value. Specifically,

$$p_\lambda = 1 - \Phi\left(\frac{\hat{\theta} - \tau}{\sqrt{\hat{\sigma}^2/N}}\right),$$

where $\hat{\sigma}^2$ is any consistent estimate of $\sigma_{\hat{y}'}^2 + \frac{1}{r} \sigma_{\hat{y}'-y'}^2$, satisfies Eq. 6. We use the estimate $\hat{\sigma}^2 = \hat{\sigma}_{\hat{y}'}^2 + \frac{N}{n} \hat{\sigma}_{\hat{y}'-y}^2$ where $\hat{\sigma}_{\hat{y}'}^2 = \frac{1}{N} \sum_{i=1}^N (g(\hat{y}'_i) - \hat{\mu}_{\hat{y}'})^2$ and $\hat{\sigma}_{\hat{y}'-y}^2 = \frac{1}{n} \sum_{j=1}^n (w_j [g(y_j) - g(\hat{y}_j)] - \hat{\Delta})^2$, which is consistent since $\hat{\sigma}_{\hat{y}'}^2$ and $\hat{\sigma}_{\hat{y}'-y}^2$ are consistent estimates of $\sigma_{\hat{y}'}^2$ and $\sigma_{\hat{y}'-y'}^2$, respectively.

Having established the validity of p_λ , $\lambda \in \Lambda$, we can control the family-wise error rate (FWER) with a Bonferroni correction:

$$\limsup_{n, N \rightarrow \infty} \text{FWER} := \limsup_{n, N \rightarrow \infty} \mathbb{P}\left(\bigcup_{\lambda \in \Lambda: \theta_\lambda < \tau} \lambda \in \hat{\Lambda}\right) \leq \sum_{\lambda \in \Lambda: \theta_\lambda < \tau} \limsup_{n, N \rightarrow \infty} \mathbb{P}(\lambda \in \hat{\Lambda}) \quad (7)$$

$$= \sum_{\lambda \in \Lambda: \theta_\lambda < \tau} \limsup_{n, N \rightarrow \infty} \mathbb{P}\left(p_\lambda \leq \frac{\alpha}{|\Lambda|}\right) \quad (8)$$

$$\leq |\{\lambda \in \Lambda : \theta_\lambda < \tau\}| \cdot \frac{\alpha}{|\Lambda|} \quad (9)$$

$$\leq |\Lambda| \cdot \frac{\alpha}{|\Lambda|} = \alpha, \quad (10)$$

where the first line uses a union bound, the second follows from the definition of $\hat{\Lambda}$ in Algorithm 1, and the third is due to the validity of each p_λ . This gives us $\liminf_{n, N \rightarrow \infty} \mathbb{P}(\theta_\lambda \geq \tau, \forall \lambda \in \hat{\Lambda}) = 1 - \limsup_{n, N \rightarrow \infty} \text{FWER} \geq 1 - \alpha$. \square

A.2 Proof of Theorem 1 (finite sample-valid design algorithm selection)

Proof. We first show that the p-value computed by Algorithm 3, p_λ , has finite-sample validity, meaning that under the null hypothesis, $H_\lambda : \theta_\lambda < \tau$, we have $\mathbb{P}(p_\lambda \leq u) \leq u, \forall u \in [0, 1]$. First, the confidence lower bound, L_α , computed by PPMEANLB (Alg. 4) is valid: it satisfies $\mathbb{P}(\theta_\lambda \geq L) \geq 1 - \alpha$. This follows from the fact that MEANLB produces valid confidence lower bounds, $\hat{\mu}_{\text{lower}}$ and Δ_{lower} , for $\mathbb{E}_{X \sim P_{X;\lambda}}[g(f(X))]$ and $\mathbb{E}_{X, Y \sim P_{X;\lambda} \cdot P_{Y|X}}[g(Y) - g(f(X))]$, respectively (Theorem 3 from Waudby-Smith and Ramdas [50]). Adding together these bounds, following the decomposition in Eq. 4, therefore yields a valid confidence lower bound, L_α , for θ_λ . Algorithm 3 then constructs a p-value by inverting L_α :

$$p_\lambda = \inf\{\alpha \in [0, 1] : L_\alpha > \tau\}. \quad (11)$$

This p-value is valid because under the null hypothesis, $H_\lambda : \theta_\lambda < \tau$, for all $u \in [0, 1]$ we have

$$\mathbb{P}(p_\lambda \leq u) \leq \mathbb{P}(\theta_\lambda < L_u) = 1 - \mathbb{P}(\theta_\lambda \geq L_u) = 1 - (1 - u) = u,$$

where the first inequality follows from the definition of p_λ in Eq. 11 and the fact that $\theta_\lambda < \tau$, and the second equality comes from the validity of L_u .

Having established the validity of $p_\lambda, \lambda \in \Lambda$, the family-wise error rate (FWER), or the probability that one or more unsuccessful configurations is selected, can be controlled with the Bonferroni correction:

$$\begin{aligned} \text{FWER} &:= \mathbb{P}\left(\bigcup_{\lambda \in \Lambda: \theta_\lambda < \tau} \lambda \in \hat{\Lambda}\right) \leq \sum_{\lambda \in \Lambda: \theta_\lambda < \tau} \mathbb{P}(\lambda \in \hat{\Lambda}) \\ &= \sum_{\lambda \in \Lambda: \theta_\lambda < \tau} \mathbb{P}\left(p_\lambda \leq \frac{\alpha}{|\Lambda|}\right) \\ &\leq |\{\lambda \in \Lambda : \theta_\lambda < \tau\}| \cdot \frac{\alpha}{|\Lambda|} \\ &\leq |\Lambda| \cdot \frac{\alpha}{|\Lambda|} = \alpha, \end{aligned}$$

where the first line uses a union bound, the second follows from the definition of $\hat{\Lambda}$ in Algorithm 1, and the third is due to the validity of each p_λ . We then have $\mathbb{P}(\theta_\lambda \geq \tau, \forall \lambda \in \hat{\Lambda}) = 1 - \text{FWER} \geq 1 - \alpha$. \square

B Extensions

B.1 More general success criteria

The main text considers success criteria of the following form: $\theta_\lambda = \mathbb{E}_{Y \sim P_{Y;\lambda}}[g(Y)] \geq \tau$ for some $g : \mathcal{Y} \rightarrow \mathbb{R}, \tau \in \mathbb{R}$. More generally, we can use prediction-powered inference techniques to compute valid p-values whenever θ_λ can be expressed as the minimizer of the expectation of some convex loss [2]:

$$\theta_\lambda = \arg \min_{\theta} \mathbb{E}_{X, Y \sim P_{X;\lambda} \cdot P_{Y|X}}[\ell_\theta(X, Y)],$$

where ℓ_θ is convex in θ . For example, when $\ell_\theta(X, Y) = (g(Y) - \theta)^2$ for some $g : \mathcal{Y} \rightarrow \mathbb{R}$, we recover the special case of $\theta_\lambda = \mathbb{E}_{Y \sim P_{Y;\lambda}}[g(Y)]$. We could not conceive of practical settings requiring the general characterization of θ_λ , but it may be useful for future work.

B.2 Design and labeled densities known up to normalizing constants

We can compute asymptotically valid p-values if we have unnormalized forms of the design and labeled densities, such as when sequences are generated from energy-based models [7], Potts models [34, 16], or other Markov random fields. Specifically, assume we can evaluate $p_{X;\lambda}^u(x) = a \cdot p_{X;\lambda}(x)$ and $p_{\text{lab}}^u(x) = b \cdot p_{\text{lab}}(x)$ for unknown constants $a, b \in \mathbb{R}$, where the superscript indicates that the densities are unnormalized. To leverage

these in place of the exact densities in Algorithm 2, consider the corresponding scaled density ratios on the labeled data, $w_j^u := p_{X;\lambda}^u(x_j)/p_{\text{train}}^u(x_j), j = 1, \dots, n$. The self-normalized importance-weighted estimate of prediction bias,

$$\hat{\Delta}^u := \frac{\sum_{j=1}^n w_j^u \cdot (g(y_j) - g(\hat{y}_j))}{\sum_{j=1}^n w_j^u},$$

is a consistent estimator of the rectifier, $\mathbb{E}_{X,Y \sim P_{X;\lambda} \cdot P_{Y|X}}[g(Y) - g(f(X))]$, just as $\hat{\Delta}$ is in Algorithm 2. Since $\hat{\Delta}^u$ is a ratio of means, the delta method can be used to derive its asymptotic distribution [29], whose variance can be estimated as

$$\hat{\sigma}_{\hat{\Delta}^u}^2 := \frac{1}{n} \frac{\frac{1}{n} \sum_{j=1}^n (w_j^u)^2 \cdot ([g(y_j) - g(\hat{y}_j)] - \hat{\Delta}^u)^2}{\left(\frac{1}{n} \sum_{j=1}^n w_j^u\right)^2}.$$

We can then compute an asymptotically valid p-value as

$$P := 1 - \Phi\left(\frac{(\hat{\theta} - \tau)}{\sqrt{\hat{\sigma}_{\hat{y}'}^2/N + \hat{\sigma}_{\hat{\Delta}^u}^2}}\right),$$

where $\hat{\theta}$ is computed using $\hat{\Delta}^u$ instead of $\hat{\Delta}$.

C Other methods

C.1 Prediction-only method

Algorithm 6 Prediction-only p-value

Inputs: Predictions for designs, $\{\hat{y}'_i\}_{i=1}^N$; desired threshold, $\tau \in \mathbb{R}$.

Output: p-value, P .

- 1: $\hat{\theta} \leftarrow \frac{1}{N} \sum_{i=1}^N g(\hat{y}'_i)$
 - 2: $\hat{\sigma}_{\hat{y}'}^2 \leftarrow \frac{1}{N} \sum_{i=1}^N (g(\hat{y}'_i) - \hat{\theta})^2$
 - 3: $P \leftarrow 1 - \Phi\left(\frac{(\hat{\theta} - \tau)}{\sqrt{\hat{\sigma}_{\hat{y}'}^2/N}}\right)$
-

The prediction-only method runs multiple testing (Alg. 1) with p-values computed using only the predicted property values of the designs (Alg. 6), treating them as if they were labels. These p-values are asymptotically valid for testing whether $\mathbb{E}_{X \sim P_{X;\lambda}}[g(f(X))] \geq \tau$ —that is, whether the expected function of *predictions* for designs, but not necessarily their labels, surpasses a threshold.

C.2 Gaussian-mixture-model forecasts method

The `GMMForecasts` method follows Wheelock et al. [52], who model the forecast for a given sequence as mixture of two Gaussians (representing beliefs over the label if the sequence is “nonfunctional” and “functional”) with sequence-specific means, variances, and mixture proportion. To construct these forecasts, the method first assumes access to a predictive mean and variance for each sequence. When using predictive models that were ensembles (i.e., the feedforward ensemble in the GB1 experiments, and the feedforward and convolutional ensembles in the RNA experiments), we set these to the mean and variance, respectively, of the predictions for a sequence. When using the ridge regression model in the RNA experiments, the model weights were fit on 90% of the training data, and the predictive mean for a sequence was set to the model’s prediction. The (homogeneous) predictive variance was set to the model’s mean squared error over the remaining 10% of the training data. Wheelock et al. [52] then use the training data to fit a mapping from these initial predictive means and variances to the Gaussian mixture model (GMM) parameters. They

also seek to address covariate shift between the design and training data by using a sequence’s edit distance from a reference training sequence (set to the wild type GB1 in the GB1 experiments, and the seed sequence in the RNA experiments) as an additional feature in fitting this mapping.

The forecasts also involve a key hyperparameter, $q \in [0, 1]$. After the GMM parameters are inferred for each design, the method adjusts the sequence-specific mean of the “functional” Gaussian by taking a convex combination of it and the original predictive mean, where q weights the latter. Using different values of q reflects how much one trusts the initial predictions; high values result in forecasts where the “functional” Gaussian mean is determined largely by the original predictive mean. We ran the method with $q \in \{0, 0.5, 1\}$ to span the range of possible values.

C.3 Calibrated forecasts method

The `CalibratedForecasts` method invokes the idea that the forecasts for sequences, or models of the conditional distributions of the label, should be statistically consistent with the true conditional distributions of the label. Specifically, we want the forecasts to be *calibrated* as defined by Kuleshov et al. [26], whose definition is related to the notion of probabilistic calibration [17]:

$$P_{X,Y}(Y \leq F_X^{-1}(p)) = p, \forall p \in [0, 1], \quad (12)$$

where F_X denotes the CDF of the forecast for a sequence $X \in \mathcal{X}$, and the probability is over the distribution of labeled data. That is, for any $p \in [0, 1]$, the label will fall under the p -quantile given by a calibrated forecast with frequency p .

For any given sequence, let an initial forecast be a Gaussian with mean and variance set to a predictive mean and variance, as described above for `GMMForecasts`. We then use the held-out labeled data to learn a transformation of these initial forecast CDFs, with the objective of achieving calibration (Eq. 12). Specifically, we use isotonic regression, following Kuleshov et al. [26]. We then construct the forecast for any given design by first forming the initial forecast, and then transforming the corresponding CDF with the fitted isotonic regression function.

C.4 Conformal prediction method

Algorithm 7 Conformal prediction-based method for design algorithm selection

Inputs: Designs generated with each configuration, $\{x_i^\lambda\}_{i=1}^N$ for all $\lambda \in \Lambda$; predictive models used by each configuration, $\{f_\lambda\}_{\lambda \in \Lambda}$; held-out labeled data, $\{(x_i, y_i)\}_{i=1}^n$; desired threshold, $\tau \in \mathbb{R}$; error rate, $\alpha \in [0, 1]$.

Output: Subset of selected configurations, $\hat{\Lambda} \in \Lambda$.

```

1: for  $\lambda \in \Lambda$  do
2:    $\hat{y}_i^\lambda \leftarrow f_\lambda(x_i^\lambda), i = 1, \dots, N$  ▷ predictions for designs
3:    $\hat{y}_j \leftarrow f_\lambda(x_j), j = 1, \dots, n$  ▷ predictions for labeled data
4:    $v_i^\lambda \leftarrow \text{DENSITYRATIO}_\lambda(x_i^\lambda), i = 1, \dots, N$  ▷ density ratios for designs
5:    $w_j^\lambda \leftarrow \text{DENSITYRATIO}_\lambda(x_j), j = 1, \dots, n$  ▷ density ratios for labeled data
6:    $l_i^\lambda \leftarrow \text{SPLITCONFORMALLB}((\hat{y}_i^\lambda, v_i^\lambda), \{(y_j, \hat{y}_j^\lambda, w_j^\lambda)\}_{j=1}^n, \alpha/(|\Lambda| \cdot N)), i = 1, \dots, N$  ▷ Alg. 8
7:    $L_\lambda \leftarrow (1/N) \sum_{i=1}^N l_i^\lambda$  ▷ average of designs’ conformal lower bounds
8: end for
9:  $\hat{\Lambda} \leftarrow \{\lambda \in \Lambda : L_\lambda \geq \tau\}$ 

```

We adapt conformal prediction techniques to conduct design algorithm selection (Alg. 7). For simplicity of exposition, we will describe the method assuming the function g is the identity; for any other function, one can replace all references to “labels” with $g(Y)$.

We first explain how to construct a valid lower bound for the empirical average of design labels, $(1/N) \sum_{i=1}^N y'_i$, for a single configuration, λ . We can use a split conformal method [47] to construct valid lower bounds, $l_i, i = 1, \dots, N$, for the labels of N designs, with confidence of $1 - \alpha/N$ each (Alg. 8). These lower bounds each satisfy $\mathbb{P}(y'_i \geq l_i) \geq 1 - \alpha/N$, where the probability is over random draws of the held-out labeled data. The

Algorithm 8 SPLITCONFORMALLB: split conformal lower bound for a design label

Inputs: a design’s prediction and density ratio, (\hat{y}', w') ; labels, predictions, and density ratios for held-out labeled data, $\{(y_j, \hat{y}_j, w_j)\}_{j=1}^n$; $\alpha \in [0, 1]$.

Output: Lower bound, $L \in \mathbb{R}$.

- 1: $u_j \leftarrow \frac{w_j}{\sum_{j=1}^n w_j + w'}$, $j = 1, \dots, n$
 - 2: $u' \leftarrow \frac{w'}{\sum_{j=1}^n w_j + w'}$
 - 3: $r \leftarrow (1 - \alpha)$ -quantile of the distribution comprising the mixture of point masses: $\sum_{j=1}^n u_j \cdot \delta_{\hat{y}_j - y_j} + u' \cdot \delta_\infty$
 - 4: $L \leftarrow \hat{y}' - r$
-

average of these bounds, $L = (1/N) \sum_{i=1}^N l_i$, is then a valid lower bound for the empirical average of design labels: $\mathbb{P}((1/N) \sum_{i=1}^N y'_i \geq L) \geq 1 - \alpha$. To see why, note that the event $\{y'_i \geq l_i, \forall i \in [N]\}$ occurs with probability at least $1 - \alpha$ due to the Bonferroni correction, and on this event, we have $(1/N) \sum_{i=1}^N y'_i \geq (1/N) \sum_{i=1}^N l_i$.

To conduct design algorithm selection, we introduce an additional Bonferroni correction for the size of the menu, $|\Lambda|$: for each design from each configuration, we construct a split conformal lower bound with a confidence of $1 - \alpha/(|\Lambda| \cdot N)$. For each configuration, we then take the average lower bound, L_λ . The additional Bonferroni correction means that the event $\{(1/N) \sum_{i=1}^N y_i^\lambda \geq L_\lambda, \forall \lambda \in \Lambda\}$ occurs with probability at least $1 - \alpha$, which in turn implies that for $\hat{\Lambda} := \{\lambda \in \Lambda : L_\lambda \geq \tau\}$, we have

$$\mathbb{P}\left(\frac{1}{N} \sum_{i=1}^N y_i^\lambda \geq \tau, \forall \lambda \in \hat{\Lambda}\right) \geq 1 - \alpha.$$

Note that the lower bounds, $L_\lambda, \lambda \in \Lambda$, are immensely conservative: because conformal prediction techniques are tailored explicitly for individual labels, not functionals of label distributions, they cannot naturally account for how signed prediction errors over many designs can “cancel out” in estimation of the mean design label. We rely instead on Bonferroni corrections to guarantee the extremely stringent criterion that each and every individual design’s lower bound is correct. In practice, this meant that L_λ was always negative infinity in our experiments. Conformal prediction is fundamentally not the right tool when one is interested in how prediction error affects distributions of labels and properties thereof, rather than just the labels of individual examples.

D Protein GB1 experiment details

Labels were a log enrichment relative to the wild type GB1, such that values greater (less) than 0 indicate greater (less) binding affinity than the wild type. Following Zhu, Brookes, & Busia *et al.* (2024), the predictive model, f , was an ensemble of feedforward neural networks trained using a weighted maximum likelihood method that accounted for the estimated variance of each sequence’s log enrichment label. After training on 5k labeled sequences, the model’s predictions for all $x \in \mathcal{X}$ yielded an RMSE of 1.02, Pearson correlation coefficient of 0.79, and Spearman correlation coefficient of 0.68 (Fig. 5).

D.1 Exceedance-based success criteria

We ran the same experiments described in §5.1, except with success criteria involving the exceedance over 1: $\mathbb{E}_{Y \sim P_{Y,\lambda}}[\mathbb{1}(Y \geq 1)] \geq \tau$, for $\tau \in [0, 1]$. For context, a label value of 1 is the 0.994-quantile of the training labels and represents a binding affinity of about 2.7 times that of wild type GB1. The results were qualitatively similar to those with success criteria involving the mean design label in the main text (Fig. 6), except that **GMMForecasts** with $q \in \{0, 0.5\}$ was slightly less conservative (though still too conservative to be useful, as it ceased selecting any temperatures for $\tau > 0.05$ and $\tau > 0.15$ for $q = 0$ and $q = 0.5$, respectively).

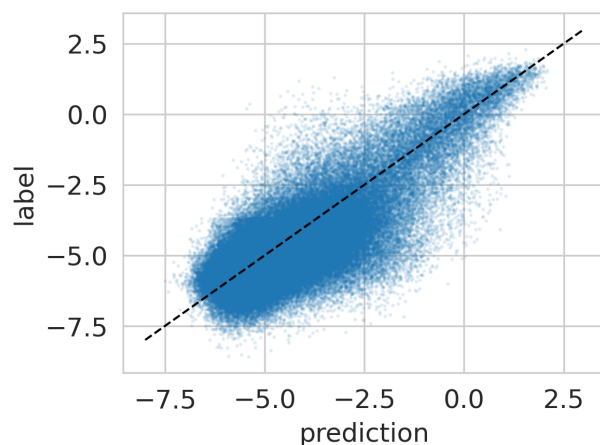


Figure 5: **Binding affinity predictions for all protein GB1 variants.** Predicted and measured binding affinity for all variants of protein GB1 at four sites of interest. Labels are from Wu et al. [53] and predictions are from an ensemble of feedforward models trained on 5k labeled sequences from the NNK library. Both axes are log enrichments relative to wild type GB1, such that the wild type has a label of 0.

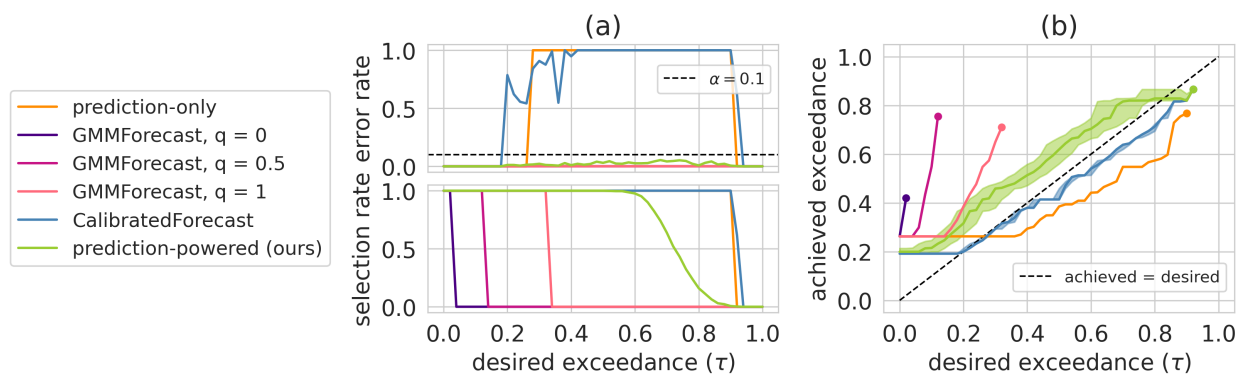


Figure 6: **Design algorithm selection for designing protein GB1.** (a) Error rate (top; lower is better) and selection rate (bottom; higher is better) for all methods, for range of values of τ , the desired exceedance over 1 (that is, the fraction of designs whose label exceeds 1). (b) Median (solid line) and 20th to 80th percentiles (shaded regions), of the lowest mean design label of selected configurations, across trials for which each method did not return the empty set. Dots mark where each median trajectory ends (i.e., the desired exceedance beyond which a method ceases to select any configuration).

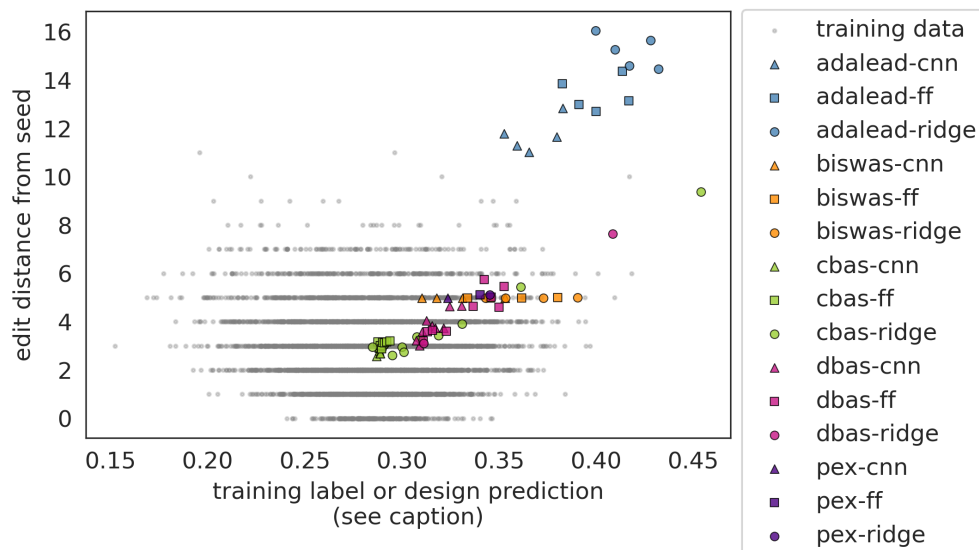


Figure 7: **Design algorithm configurations for designing RNA binders.** Gray dots give the label (x -axis) and edit distance from a seed sequence (y -axis) for the 5k training sequences used by the predictive models. Colored markers give the average design prediction (x -axis) and average edit distance from the seed (y -axis) for each configuration on the menu. Multiple colored markers of the same type correspond to different hyperparameter settings; for example, the five blue triangles correspond to `AdaLead-CNN-0.2`, `AdaLead-CNN-0.15`, `AdaLead-CNN-0.1`, `AdaLead-CNN-0.05`, and `AdaLead-CNN-0.01`.

E RNA binder experiment details

To facilitate interpretability of the label values, following Sinai et al. [40] we normalized the ViennaFold binding energy [28] by that of the complement of the RNA target sequence, which can be seen as an estimate of the energy of the true optimal binding sequence. Consequently, a label value of 1 means a binding energy equal to that of the complement sequence.

E.1 Menu of design algorithm configurations

Predictive models. The three predictive models were a ridge regression model, where the ridge regularization hyperparameter was set by leave-one-out cross-validation; an ensemble of three feedforward neural networks, each with two 100-unit hidden layers; and an ensemble of three convolutional neural networks, each with three convolutional layers with 32 filters, followed by two 100-unit hidden layers. Each model in both ensembles was trained for five epochs using Adam with a learning rate of 10^{-3} .

Design algorithm hyperparameter settings. For `AdaLead` [40], the values of the threshold hyperparameter on the menu were $\kappa \in \{0.2, 0.15, 0.1, 0.05, 0.01\}$. For `Biswas`, the algorithm used by Biswas et al. [7], the values of the temperature hyperparameter on the menu were $T \in \{0.02, 0.015, 0.01, 0.005\}$. For `Conditioning by Adaptive Sampling` [8], or `CbAS`, the values of the quantile hyperparameter on the menu were $Q \in \{0.1, 0.2, \dots, 0.9\}$. For `Design by Adaptive Sampling` [9] (`DbAS`) with either the FF or CNN models, the values of the quantile hyperparameter on the menu were $Q \in \{0.1, 0.2, \dots, 0.9\}$, and with ridge regression, $Q \in \{0.1, 0.2\}$. Both `CbAS` and `DbAS` involve a generative model, which was a variational autoencoder (VAE) with 10 latent dimensions, and feedforward models with 20-unit hidden layers for both the encoder and decoder. Both algorithms were run for twenty iterations; each iteration retrained the VAE for five epochs using Adam with learning rate 10^{-3} . `PEX` [31] was run with default values of all hyperparameters. The resulting menu of design algorithm configurations varied greatly in their the mean design prediction, as well

as their deviation from the training sequences (Fig. 7).

E.2 Density ratio estimation

To estimate the density ratio function, $p_{X;\lambda}(\cdot)/p_{\text{lab}}(\cdot)$, for every configuration on the menu, $\lambda \in \Lambda$, we used multinomial logistic regression-based density ratio estimation (MDRE) [44]. MDRE builds upon a formal connection between density ratio estimation (DRE) and classification [6, 22]: for the (correctly specified) binary classifier that minimizes the population cross-entropy risk in distinguishing between samples from two distributions, its logit for any input is equivalent to the density ratio at that input [22]. In practice, however, given finite samples from the two distributions, we can only hope to find a classifier that minimizes the empirical risk. This distinction between the population and empirical risks hinders DRE far more than it does classification for classification’s sake: obtaining the density ratio requires getting the exact value of the population-optimal classifier’s logit, whereas optimal classification performance can be achieved by any classifier that learns the same decision boundary as the optimal classifier, even if its logits differ for some inputs. Accordingly, we found that for many configurations on the menu, classifiers with very low training and validation losses often yielded poor approximations of the density ratio. This was particularly true when the design and labeled distributions were far apart, because the classification problem is too easy given finite samples: many different classifiers can minimize the empirical risk, none of which may happen to coincide with the population-optimal one whose logits are equivalent to density ratios. Telescoping density ratio estimation [32] tackles this problem by constructing intermediate distributions that interpolate between the numerator and denominator distributions, creating a sequence of “harder” binary classification problems for which there are fewer empirically optimal classifiers, and whose resulting estimated density ratios can be combined with a telescoping sum to approximate the original density ratio of interest. MDRE is similarly motivated but constructs a single multi-class classification problem between the intermediate distributions, justified by theoretical connections between the population-optimal classifier and the density ratio analogous to those described above [44]. Concretely, let $h^c(x)$ denote the unnormalized log-probability according to a trained classifier that x belongs to distribution $c \in \{1, \dots, C\}$, where C denotes the total number of distributions. MDRE uses $\exp(h^i(x) - h^j(x))$ to approximate the density ratio between distributions i (numerator) and j (denominator).

Note that the design algorithm selection problem naturally lends itself to the construction of the intermediate distributions used by MDRE, because many design algorithms have hyperparameters that navigate how far the design distribution strays from the labeled distribution. It is often of interest to include different settings of such hyperparameters on the menu, in which case all of these configurations’ density ratios with the labeled distribution can be approximated with a single MDRE model. For the RNA binder experiments, denote by [design algorithm]-[predictive model]-[hyperparameter value] the configuration of running the specified design algorithm with the specified predictive model and hyperparameter value—for example, **Biswas-CNN-0.02** refers to running the **Biswas** design algorithm with the convolutional ensemble predictive model and temperature hyperparameter $T = 0.02$. We fit a separate MDRE model for each combination of a design algorithm and a predictive model—that is, a separate multi-class classifier for **AdaLead-ridge-***, for **AdaLead-FF-***, for **AdaLead-CNN-***, for **Biswas-ridge-***, for **Biswas-FF-***, for **Biswas-CNN-***, for **CbAS-ridge-***, for **CbAS-FF-***, for **CbAS-CNN-***, for **DbAS-ridge-***, for **DbAS-FF-***, for **DbAS-CNN-***, for **PEX-ridge**, for **PEX-FF**, and for **PEX-CNN**, where the last three reduced to binary classification problems. Each of these classifiers was fit on the 5k training sequences and $N = 50\text{k}$ design sequences from each included configuration. For example, the 10-category classifier for estimating density ratios **CbAS-ridge-*** was fit on 5k training sequences and 50k sequences each from **CbAS-ridge-0.1**, **CbAS-ridge-0.2**, \dots , **CbAS-ridge-0.8**, and **CbAS-ridge-0.9**. Each classifier was a model with one 256-unit hidden layer and a quadratic final layer, trained for 100 epochs using Adam with a learning rate of 10^{-3} .